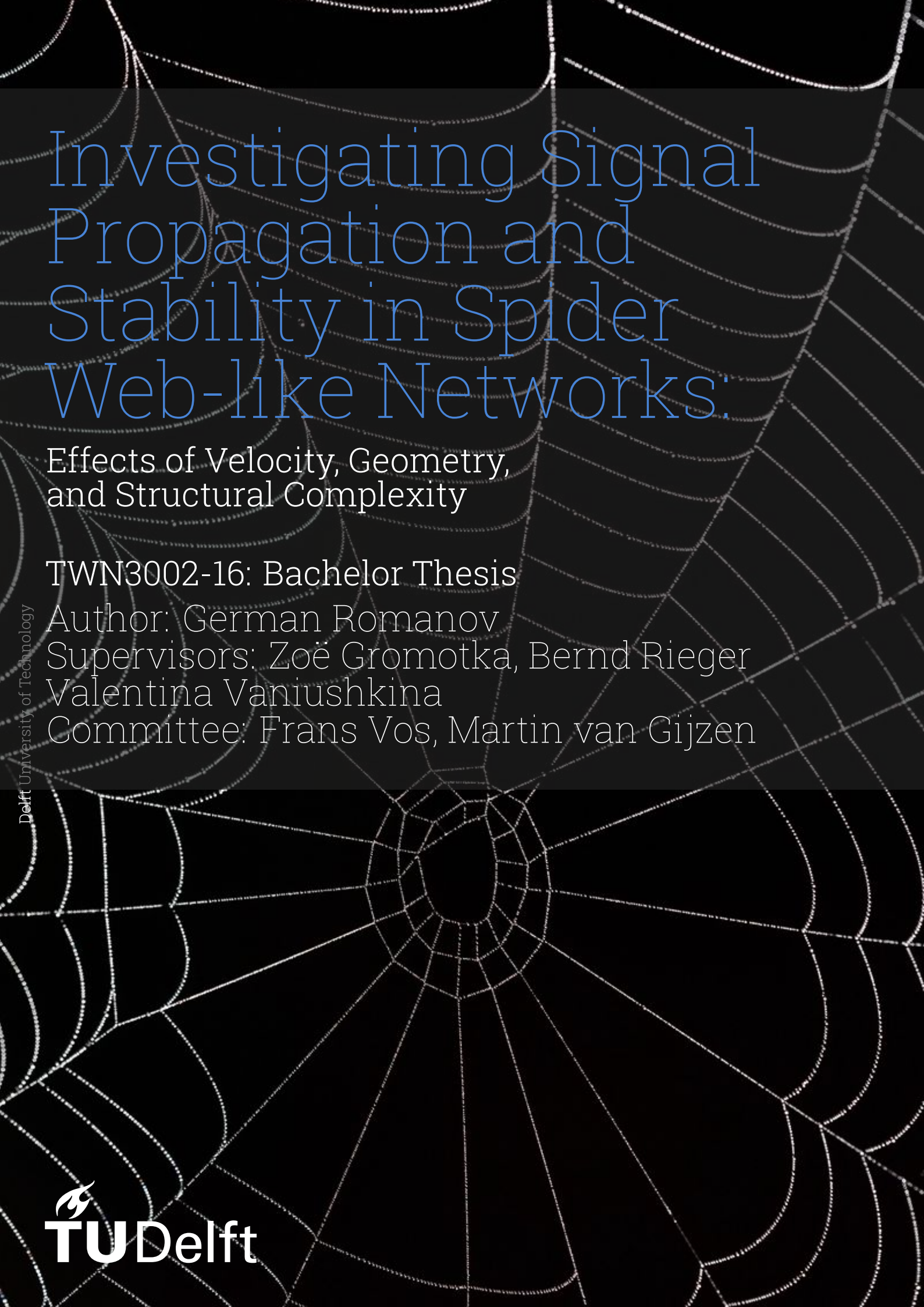

Investigating Signal Propagation and Stability in Spider Web-like Networks:

Effects of Velocity, Geometry, and Structural Complexity

TWN3002-16: Bachelor Thesis

Author: German Romanov
Supervisors: Zoë Gromotka, Bernd Rieger
Valentina Vaniushkina
Committee: Frans Vos, Martin van Gijzen

Delft University of Technology

TU Delft

Investigating Signal Propagation and Stability in Spider Web-like Networks:

Effects of Velocity, Geometry, and Structural Complexity

by

German Romanov

Student : 5279607

Instructor:	Zoë Gromotka
Teaching Assistant:	Valentina Vaniushkina
Project Duration:	Feb, 2024 - Feb, 2025
Faculty:	EEMCS, TN, Delft

TU Delft

Abstract

This thesis investigates signal propagation and stability in spider web-like networks, focusing on how velocity differences, structural geometry, and complexity influence network behavior. Spider webs, known for their resilience, flexibility, and efficient vibration transmission, offer valuable insights into designing robust artificial networks. By employing mathematical and physical modeling, this study explores force distribution, signal propagation dynamics, and collision phenomena within these networks.

The study introduces distinct propagation approaches, ranging from simple discrete collision analysis to advanced continuous simulations incorporating energy dissipation, adaptive weighting, and refined collision detection algorithms. Key methodologies include simulations of force distribution using recurrence relations, random walk models, and wavefront propagation models to examine how signals traverse complex network topologies. These simulations reveal that network topology significantly impacts signal efficiency, propagation speed, collision frequency, and signal loss, with central nodes emerging as critical hubs of activity and congestion. Additionally, structural defects such as inactive nodes, altered masses, and weakened edges are systematically introduced to evaluate their influence on the overall stability and signal propagation efficiency. These imperfections profoundly affect network performance, demonstrating the necessity for structural adaptability and redundancy to maintain integrity under stress.

Contents

1

Introduction

In recent years, network structures have gained significant attention due to their applications in communication, biology, architecture, and neural networks. To enhance network efficiency, robustness, and adaptability, understanding signal propagation is crucial. Among various network types, spider webs stand out for their strength, flexibility, and adaptability—features refined through millions of years of evolution. Their radial and spiral thread structure provides an effective model for studying signal stability and transmission, directly informing research on signal distribution, collision dynamics, and propagation efficiency.

Natural spider webs are both lightweight and highly efficient in handling stress and adapting to environmental changes(Han et al., 2021[1]. They consist of two primary thread types: radial threads, which provide structural stability, and spiral threads, which capture prey and absorb vibrations(Oxford University, 2020 [2]). This combination allows the web to function reliably even when damaged, making it an excellent model for resilient network structures.

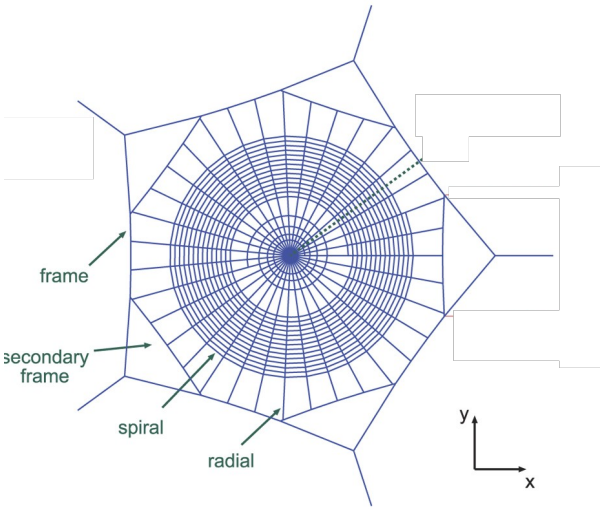

Figure 1.1: A sketch of a simplified spider web with defenitions.

Previous studies (e.g., Cranford et al., 2012 [3]) on spider web mechanics have focused on their physical properties, such as force distribution, stress tolerance, and damage resilience. Research has shown that spider webs can localize and redistribute stress, an uncommon feature in artificial materials. The hierarchical web structure enables it to withstand localized damage without compromising overall integrity. These insights are valuable for designing artificial networks with high resilience, applicable in sensor arrays, communication systems, and biomimetic designs.

Building on this foundation, this thesis explores spider web mechanics as a model for signal propagation and stability in network structures. By analyzing parameters such as node geometry, thread propagation velocities, and network complexity, this study contributes to network theory and its practical applications. Biological systems like spider webs exemplify evolved designs that combine strength, flexibility, and efficient signal transmission, providing insights for developing robust network structures.

A key aspect of spider web functionality is the distinction between its radial and spiral threads. Radial threads form the structural framework, while spiral threads assist in force dissipation. This dynamic arrangement enables efficient distribution of forces and vibrations, minimizing damage and maintaining functionality under stress. Similarly, optimized networks should aim to preserve signal stability and limit interference despite structural disruptions.

The potential applications of spider web-like network models extend to engineering and technology. Understanding how geometry and structural complexity affect signal propagation can enhance sensor networks, where reliable communication across nodes is essential. Additionally, insights from this research could improve communication networks by reducing signal collisions and interference.

This thesis addresses the overarching question: How do the structural properties and complexity of lattice frameworks—both general lattice structures and spider web-like lattices—influence signal transmission characteristics, including efficiency, propagation speed, collision frequency, and signal loss? Additionally, it explores how these effects change when structural defects are introduced.

To refine this inquiry, three key sub-questions are considered: How do signal transmission properties—efficiency, propagation speed, collision frequency, and signal loss—differ between general lattice structures and spider web-like lattices? How does increasing structural complexity within both lattice types affect signal propagation efficiency and signal loss? How do structural defects, such as broken links, missing nodes, or weakened segments, influence signal propagation in both lattice frameworks, and how do these effects differ between them?

The structure of this thesis is organized as follows: Chapter 1 introduces the research context, detailing the motivations and the primary and sub-research questions that guide this study. Chapter 2 provides a comprehensive Literature Review, synthesizing prior research on lattice structures, spider web mechanics, and signal propagation, which form the theoretical foundation for this work. Chapter 3 focuses on the Mathematical Model, presenting the formulation of both general lattice and spider weblike networks and outlining the parameters and equations governing signal propagation within these structures. Chapter 4 covers Simulation and Analysis, describing the experimental setup, variations in complexity and defect scenarios, and the results obtained from numerical and analytical methods. Chapter 5 offers a Discussion, interpreting the results in relation to the research questions, comparing the findings across lattice types, and exploring their broader implications. Finally, Chapter 6 concludes the thesis by summarizing the key contributions, identifying overarching trends, and suggesting directions for future research, including potential applications and further exploration of time-dependent or environmental factors affecting signal propagation.

2

Literature Review

As mentioned spider webs are remarkable natural structures that have evolved over millions of years to fulfill the dual purposes of capturing prey and withstanding environmental stresses(in the context of a spider web, stress refers to the internal forces per unit area generated within the web threads when subjected to external loads, such as the impact of prey, wind, or environmental disturbances). In this chapter, we review two complementary lines of research. Section 2.2 focuses on the static mechanical properties, force distribution, and design principles as presented by Aoyanagi and Okumura [4]. Section 2.3 then explores the dynamic vibrational behavior and prey localization mechanisms as investigated by Lott et al. [5]. Finally, Section 2.4 summarizes these insights and connects them to the broader context of signal propagation in spider web-like networks.

2.1. Mechanics of Spider Webs: Static Analysis - Structural Design

Introduction to Spider Web Structures and Mechanics

As mentioned spider webs are remarkable natural structures that have evolved over millions of years to fulfill the dual purposes of capturing prey and withstanding environmental stresses. The structural design of spider webs, particularly orb webs, combines resilience and flexibility, making them ideal for studying principles of stability and adaptability. Unlike many man-made materials, spider webs can maintain functionality even when parts of the structure are damaged . This unique resilience is attributed to the intricate arrangement of radial and spiral threads, each contributing differently to the web's overall strength and flexibility (Aoyanagi and Okumura, 2010)[4].

Overview of the Mechanical Properties of Orb Webs

Aoyanagi and Okumura's study, *"Simple Model for the Mechanics of Spider Webs"*, provides a foundational model for analyzing the mechanical properties of orb webs. The model simplifies the complex structure of orb webs into a two-dimensional framework, allowing for a formal analytical approach. By focusing on the interaction between radial and spiral (Figure 2.1) threads, the model sheds light on how spider webs distribute forces, resist damage, and maintain stability even under stress.

Orb webs are characterized by a central hub connected to radial threads, which are linked by spiral threads. Radial threads, stronger and stiffer, provide structural support, while spiral threads, more flexible, absorb and dissipate forces. This dual-thread structure enables the web to balance rigidity with flexibility .

A key concept in Aoyanagi and Okumura's model is the **spring constant ratio**, denoted as K/k, which represents the relative stiffness of radial and spiral threads. This ratio significantly influences force distribution throughout the web, affecting its resilience. When K/k is high (indicating stiffer radial threads), the web handles force without stress concentrations a common weakness in conventional materials. n nature, the typical ratio K/k is around 10. If this ratio is lower, the web's ability to effectively capture and distribute stress deteriorates. Thus, maintaining the correct K/k ratio is crucial for both structural stability and functionality of spider webs.

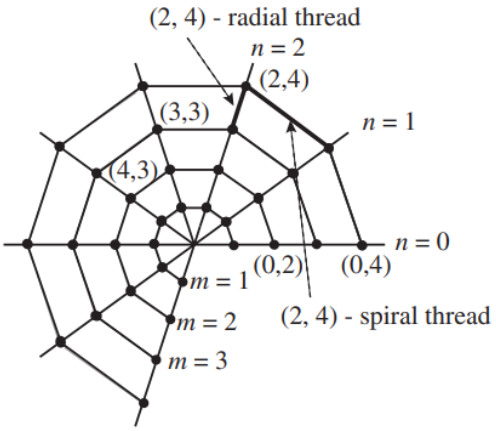

Figure 2.1: Model of orb web of spider consisting of 10 radial threads and 4 spiral threads (N = 10, M = 4), which are labeled as above(Aoyanagi and Okumura, 2010) [4].

The natural length of each spiral thread, l_m, is given by:

$$l_m = \alpha m L = 2mL \sin\left(\frac{\pi}{N}\right)$$

where L is the natural length of the radial threads, m indexes the spiral threads, N is the total number of radial threads, and α is a constant related to the web's geometry. The coordinates of the nodes, without any tension, are defined as:

$$X_{n,m} = \left(\frac{2\pi n}{N}, mL\right)$$

where n represents the radial position, and m represents the spiral position.

Damage Tolerance and Force Distribution in Spider Webs

One of the model's notable aspects is its analysis of damage tolerance. In typical materials, damage leads to stress concentrations near the damaged area, potentially compromising the entire structure. However, spider webs, particularly orb webs, show a different response. When specific spiral threads are removed or damaged, the load-bearing radial threads maintain the web's structural integrity, preventing stress concentrations from forming. This quality allows the web to remain functional despite partial damage.

The model calculates the forces acting on each thread, showing that force accumulates toward the radial threads at the web's periphery. The force on each radial thread F_m and each spiral thread f_m is calculated using the following recurrence relation:

$$\frac{F_{m+1}}{\tilde{k}_{m+1}} = \left(\frac{1}{\tilde{k}_{m+1}} + \frac{1}{\tilde{k}_m} + \frac{\alpha^2}{K}\right) F_m - \frac{F_{m-1}}{\tilde{k}_m}$$

where $\tilde{k}_m = \frac{k}{l_m}$ represents the spring constant per unit length for the m-th spiral thread, and K is the spring constant of the radial threads. The initial conditions for force calculations are defined as:

$$F_1 = \tilde{K}\Delta L, \quad f_1 = \alpha \tilde{k}_1 \Delta L$$

where ΔL is the elongation of the first radial thread.

To simulate damage, the model removes specific spiral threads and recalculates the force distribution. The absence of a spiral thread alters local force distribution, but the overall structure remains free from stress concentrations due to the strength and configuration of radial threads.

Design Principles and Broader Implications

The damage tolerance and stress distribution characteristics of spider webs offer valuable design principles for modern engineering applications. The insights from spider web mechanics can inform the design of structures that are both resilient and adaptable. Some potential applications include:

- **Buildings**: Using spider web principles to enhance structural integrity and damage tolerance in architectural designs.
- **Bridges**: Applying the web's force distribution characteristics to improve bridge resilience under load.
- **Space Structures**: Leveraging damage tolerance and stress distribution in designing space structures that withstand environmental stresses.
- **Material Science**: Developing new materials that mimic spider web resilience for enhanced damage tolerance.
- **Biomimicry**: Exploring how spider web-inspired structures can drive innovation in engineering solutions, such as in sensor networks or load-bearing structures.

The model developed by Aoyanagi and Okumura provides a strong foundation for understanding these design principles. The web's hierarchical structure—where strong radial threads are supported by flexible spiral threads—serves as a model for creating resilient networks and materials that can withstand variable stresses without failure. An appropriately large K/k ratio, as observed in real spider webs, significantly enhances damage tolerance by minimizing stress concentrations. The findings highlight general physical principles that could be beneficial for designing resilient artificial structures and materials.

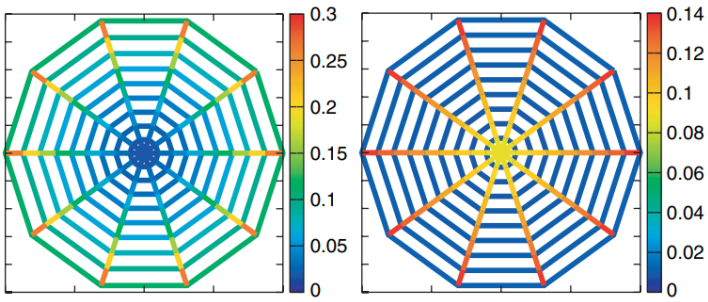

Figure 2.2: Force distribution in undamaged spider web models for different stiffness ratios between radial and spiral threads. The left image shows a web with a stiffness ratio of $K/k = 1$, representing an evenly distributed force network, where the force concentration is spread more uniformly, resulting in moderate force values across the web. In contrast, the right image depicts a web with a stiffness ratio of $K/k = 10$, which more closely corresponds to natural spider webs where radial threads are significantly stiffer than spiral threads (Aoyanagi and Okumura, 2010)[4].

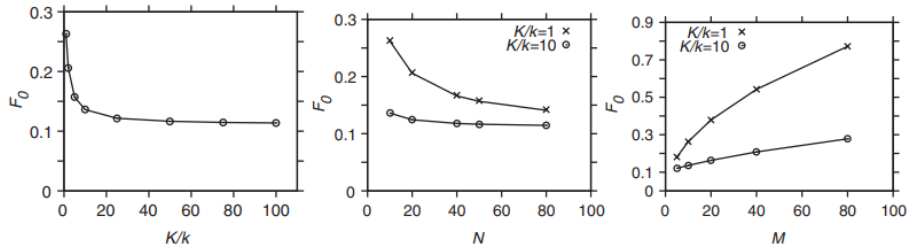

Figure 2.3: Plots showing the maximum force F_0 (in $\tilde{K}\Delta$) in the spider web model under different parameters. The left plot illustrates F_0 as a function of the stiffness ratio K/k for a web with $N = 10$ radial threads and $M = 9$ spiral threads. As K/k increases, F_0 decreases, indicating that a higher stiffness ratio leads to more effective force distribution. The middle plot shows F_0 as a function of the number of radial threads N for two stiffness ratios, $K/k = 1$ and $K/k = 10$, with $M = 9$ spiral threads. The right plot presents F_0 as a function of the number of spiral threads M for $N = 10$ radial threads, comparing $K/k = 1$ and $K/k = 10$. Here, F_0 increases with M, especially for higher K/k ratios, indicating that adding spiral threads increases the load on individual radial threads when radial threads are much stiffer than spiral thread (Aoyanagi and Okumura, 2010)[4].

2.2. Vibrational Analysis and Prey Localization in Spider Webs

A complementary study by Lott et al., titled *"Prey Localization in Spider Orb Webs Using Modal Vibration Analysis"* (Lott et al., 2022)[6], explores how spiders use their webs to detect and locate prey based on vibrational signals. This research provides essential insights into the mechanics of signal propagation and detection in spider webs, emphasizing how vibration patterns can encode information about the location of impacts. The study uses modal analysis to reveal how different frequencies and modes contribute to prey detection, making it relevant for understanding signal propagation in spider web-like networks.

2.2.1. Spider Web Geometry and Modal Vibration Analysis

The model used in this study considers an asymmetric orb web with an octagonal structural frame. Radial threads connect to this frame, while spiral threads are arranged in a spiral pattern starting from an off-center hub. This geometry closely reflects the realistic structure of natural orb webs. Prior to analyzing vibrations, the web is prestressed by applying forces from the center outward, ensuring equilibrium and preventing rigid-body motion. The prestressed configuration introduces high levels of tension, particularly in the radial threads, which influences the web's vibrational behavior and sensitivity to impacts (Lott et al., 2022)[6].

To understand how spiders detect vibrations, the study (Lott et al., 2022)[6] performs eigenfrequency analysis on the prestressed web to identify its resonant frequencies and corresponding modal shapes. Modal decomposition breaks down complex vibration patterns into simpler components, or eigenmodes, revealing the characteristic ways in which the web oscillates in response to disturbances. These modal shapes help identify how the web vibrates and responds to impacts at specific frequencies, allowing spiders to detect and localize prey .

The spider's ability to detect prey is modeled by treating its legs as independent sensors that pick up vibrations. These vibrations can be used to determine the location of the source. In the research, the Green's function is applied for vibration analysis. The analysis shows that higher modes provide sufficient resolution for accurate prey detection, while lower modes, such as the fundamental mode, are less effective for precise localization.

2.2.2. Mathematical Model: Resonant Frequency and Green's Function

The resonant frequency f_0 of a web thread under tension is given by:

$$f_0 = \frac{1}{2L}\sqrt{\frac{T}{\rho l}}$$

where:

- L is the length of the thread,
- T is the tension in the thread, and
- ρl is the mass per unit length of the thread.

This formula indicates that the resonant frequency increases with greater tension or shorter length.

The study further examines the **Variation of Resonant Frequency** when the web is subjected to additional pulling forces. The resonant frequency f_0 changes according to:

$$\frac{\delta f_0}{f_0} = -\frac{\delta L}{L} + \frac{1}{2}\frac{\delta T}{T}$$

where:

- δL and δT represent small changes in the length and tension, respectively.

This equation reflects two opposing effects: increasing tension raises the resonant frequency, while increasing length decreases it.

To model how vibrations propagate across the web, the study uses **Green's Function**, which describes how a disturbance (such as an impact) at one point on the web propagates to another point:

General formula defined by

$$LG(x,s) = \delta(x-s)$$

$$G(x,s) = \sum_n \frac{\phi_n(x)\phi_n(s)}{\lambda_n}$$

explaining web nodes:

$$G_{ij}(x,s) = \phi_{in}(x)\phi_{nj}(s)^\dagger$$

where:

- ϕ_{in} represents the mode shape at point i for mode n, and
- $\phi_{nj}^\dagger$ is the complex conjugate transpose of the mode shape at point j.

Each vibration mode of the web corresponds to a specific eigenshape, defining how the web deforms at different frequencies. When prey impacts the web, it excites a combination of these modes, generating a unique vibration pattern based on the disturbance location. The spider detects these mode contributions at its contact points, using phase and amplitude differences to precisely locate the prey

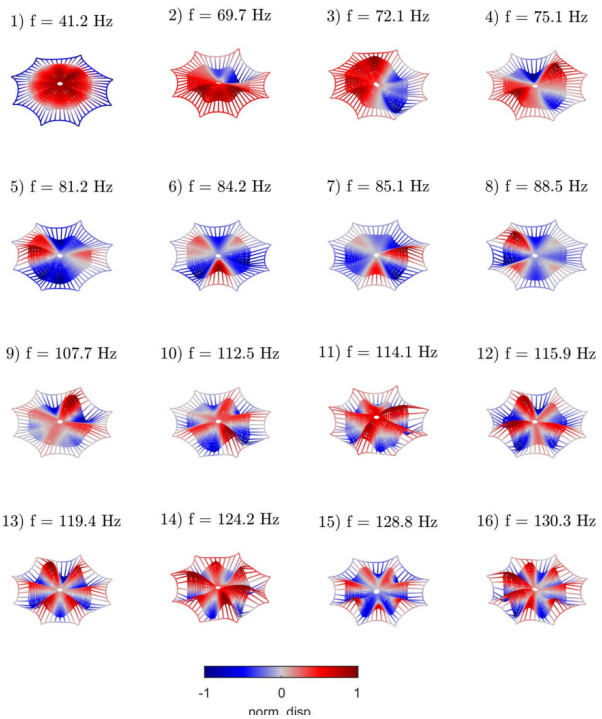

Figure 2.4: Vibration eigenmodes of the spider web, modeled by pre-stressed trusses with geometrical nonlinearity (Lott et al., 2022)[6].

2.2.3. Application of Findings for Signal Propagation in Artificial Networks

The findings of Lott et al. demonstrate that spider webs function as highly tuned vibrational networks capable of distinguishing between various types of impacts. The concept of using modal decomposition and Green's function for source localization has implications for artificial networks that require impact detection and localization. The principles of prestressed structure and vibration analysis could be adapted to enhance the design of networks that need precise impact detection, such as sensor networks or structural health monitoring systems.

The insights from this study provide valuable background for understanding how signal propagation in spider web-like networks can be modeled. By applying concepts from modal analysis and Green's functions, this thesis can investigate how artificial networks might use structural geometry and vibrational sensitivity to enhance stability and signal accuracy. Additionally, the use of Green's function and modal imaging offers a framework for exploring collision frequency and propagation delay in spider web-like networks, extending the principles of natural systems to engineered applications.

2.3. Summary and Connection to the Rest of the Work

The studies by Aoyanagi and Okumura and by Lott et al. collectively offer a comprehensive framework for examining the static mechanics with vibrational behavior of spider webs. The static mechanical models reveal how spider webs distribute forces and tolerate damage through a hierarchical structure of strong radial and flexible spiral threads. Meanwhile, the vibrational analysis demonstrates how modal decomposition, resonant frequency variation, and Green's function enable precise prey localization and offer insights into signal propagation. These combined insights form the basis for extending the natural principles observed in spider webs to the design of artificial networks. In the following chapters, this thesis will build on these principles to investigate novel methods for enhancing stability, reducing collision frequency, and minimizing propagation delays in communication and sensor networks inspired by spider web architectures.

3

Methodology of the Structure Models

In this chapter, we introduce and develop a comprehensive framework for studying force distribution, signal propagation, and structural dynamics in spider web-like networks. We begin by outlining the mathematical and physical models drawn from literature, proceed with detailed simulation setups in Python, and then extend the approach to more advanced models that incorporate collision dynamics, defects, and force propagation. This integrated narrative connects theoretical derivations to computational experiments, culminating in advanced analyses that aim to bridge biology-inspired models and engineering applications.

The development of the model was carried out in three stages, each progressively expanding on the complexity of the network and the simulation of signal propagation

3.1. Setup of Mathematical and Physics Model From The Literature

The mathematical model used in this study is based on a network of radial and spiral threads, inspired by the structural organization of natural spider webs. This model provides a framework for examining force distribution, signal propagation, and stability within a spider web-like network. By analyzing the forces in the network, we can understand how signal collisions, propagation delays, and stability are influenced by the web's structural characteristics.

3.1.1. Basic Recurrence Relation for Force Distribution

The primary recurrence relation in this model describes the force F_{m+1} in the radial threads at successive nodes m. This recurrence relation takes into account the spring constants of the spiral threads connecting nodes m and $m+1$ and is expressed as follows:

$$\frac{F_{m+1}}{\tilde{k}_{m+1}} = \left(\frac{1}{\tilde{k}_{m+1}} + \frac{1}{\tilde{k}_m} + \frac{\alpha^2}{K}\right) F_m - \frac{F_{m-1}}{\tilde{k}_m}$$

where:

- $\tilde{k}_m$ and $\tilde{k}_{m+1}$ are the spring constants of the spiral threads between nodes m and $m+1$,
- K is the spring constant of the radial threads, assumed to be significantly larger than the spring constants of the spiral threads, and
- α is a parameter that modulates the effect of spring constants on the force distribution.

This recurrence relation shows how forces propagate from one node to the next, with the force in a radial thread at node $m+1$ depending on the forces at nodes m and $m-1$. A higher value of α increases the impact of the spring constants, potentially altering the force distribution across the web.

3.1.2. Initial Force Conditions

The initial forces in the radial and spiral threads, F_1 and f_1, respectively, are determined by the tension applied during web construction. These initial conditions are defined as:

$$F_1 = \tilde{K}\Delta L, \quad f_1 = \alpha \tilde{k}_1 \Delta L$$

where ΔL represents the initial elongation of the threads due to tension, and $\tilde{K}$ is the effective spring constant of the radial threads.

3.1.3. Reformulating the Main Equations

From the basic recurrence relation, we can rewrite the main equations as:

$$F_{m+1} = F_{m-1} + \alpha \left(f_{m-1} + f_m\right)$$
$$F_{m+1} = F_m + \alpha f_m$$

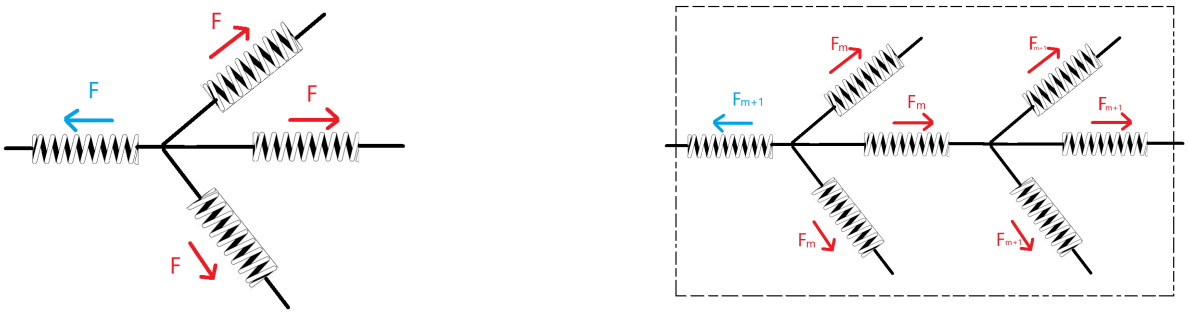

Figure 3.1: two interconnected spring systems with forces applied at various nodes. On the left side, there is a single central node connected to four springs. A blue force labeled F points to the left on the horizontal spring, while three red forces, also labeled F, point outward from the node along the other springs in different directions. On the right side, the system extends into a repeating triangular pattern, with multiple nodes and springs forming a network. The forces are labeled F_m F_{m-1} , and F_{m+1}, indicating sequential force distribution throughout the network. A blue force F_{m+1} points leftward on the leftmost spring, while red forces F_m and F_{m-1} act outward from the nodes. The dashed box outlines a repeating unit, suggesting a modular structure within the network.

These equations highlight the additive nature of the forces, where each successive radial thread force depends on the sum of the forces at previous nodes. The parameter α modulates the influence of the spiral forces on the radial forces, contributing to the overall force distribution pattern in the web.

3.1.4. Force Distribution in the Undamaged Web

In the undamaged state, the force in the radial threads accumulates toward the periphery of the web. This pattern is a result of the additive force propagation described by the recurrence relation. Increasing the ratio K/k (the stiffness ratio of radial to spiral threads) reduces the maximum force in the web, distributing the load more evenly and enhancing the web's damage tolerance. Since radial threads are stiffer (with larger K), they can carry more force without significant deformation, allowing the web to resist external stress effectively.

3.1.5. Wave Speed and its Dependence on the Medium

The speed of a wave, or signal, within the web depends on the properties of the medium, specifically the tension in the threads and their linear density. This concept is similar to the way sound is produced in musical instruments, such as a guitar, where the vibration frequency depends on the string tension and density. In the web, magnitude of the speed of signal propagation $|v|$ is given by:

$$|v| = \sqrt{\frac{F_t}{\mu}}$$

where:

- F_t is the tension mentioned in the Literature ,
- μ is the mass per unit length of the thread.

This equation indicates that the speed of the wave increases with higher tension or lower mass per unit length. It's important to note that the velocity of the signal is not influenced by the mass of an external object, such as a fly, that may impact the web; instead, it is governed by the intrinsic properties of the web itself, particularly the tension.

3.1.6. Biological Context: Characteristics of Flies as Prey

For context, flies belong to the order Diptera, derived from the Greek words 'di' meaning 'two' and 'pteron' meaning 'wing' ("Dipteran," in Merriam-Webster.com)[7]. These insects use only a single pair of wings for flight, while the hindwings have evolved into advanced mechanosensory organs known as halteres, which help them with balance and movement ("Order Diptera," in General Entomology)[8] . The average weight of a common house fly (*Musca domestica*) is approximately 12 milligrams ("Musca domestica," in Animal Diversity Web)[9]. Understanding the characteristics of prey, such as flies, helps contextualize the types of vibrations and frequencies that a spider web would typically experience, influencing the design and parameters of our model.

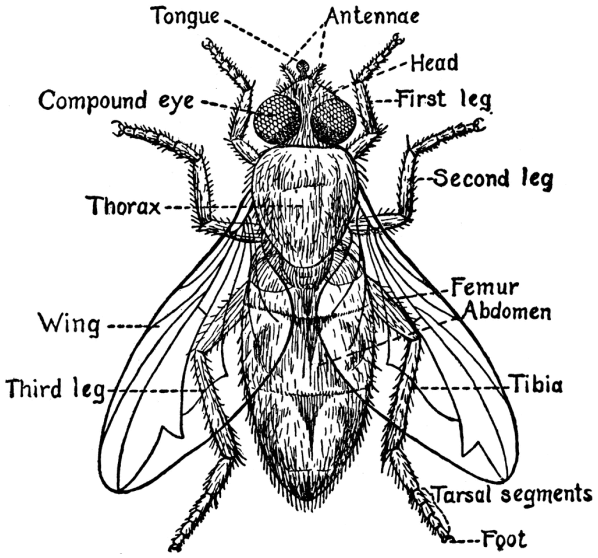

Figure 3.2: Parts of a fly structure that are labeled. (Ellsworth D. Foster ed. The American Educator (vol. 4) (Chicago, IL: Ralph Durham Company, 1921)

3.2. Three Stages of the Model

Stage 1: Structural Simulation

To begin the exploration of signal propagation in spider web-like networks, it is essential to recreate the algorithm derived from the force distribution equations mentioned earlier. This provides a foundation for calculating forces in a symmetric web, which will serve as a reference model for future studies. It is important to note that the force distribution calculated here applies strictly to symmetric webs; in asymmetric or irregular webs, the force distribution would vary significantly.

The model focuses on the fundamental requirements to simulate the spider web structure itself. It fully implements the theoretical equations described earlier into code and calculates the force distribution for a symmetric web. Using the recurrence relations, the model computes the forces in the radial and spiral threads to verify the theoretical predictions.

To calculate the forces in a symmetric spider web, we use the recurrence relation for radial thread forces, as described earlier where:

- $\tilde{k}_m = \frac{k}{l_m}$ is the spring constant per unit length of the spiral thread,
- K is the spring constant of the radial threads,
- α is a scaling factor accounting for the relative influence of spiral threads.
- $\bar{K} = 1.0\,\frac{\mathrm{N}}{\mathrm{m}}$: Stiffness of the radial threads.
- $L = 1.0\,\mathrm{mm}$: Natural length of the radial threads.
- $\Delta = 0.1\,\mathrm{mm}$: Elongation of the threads under tension.
- $K = 31.5 \times 10^{-3}\,\mathrm{N}$: Stiffness of radial threads (converted from millinewtons).
- $k = 2.26 \times 10^{-3}\,\mathrm{N}$: Stiffness of spiral threads (converted from millinewtons).
- $N = 10$: Number of radial threads in the web.

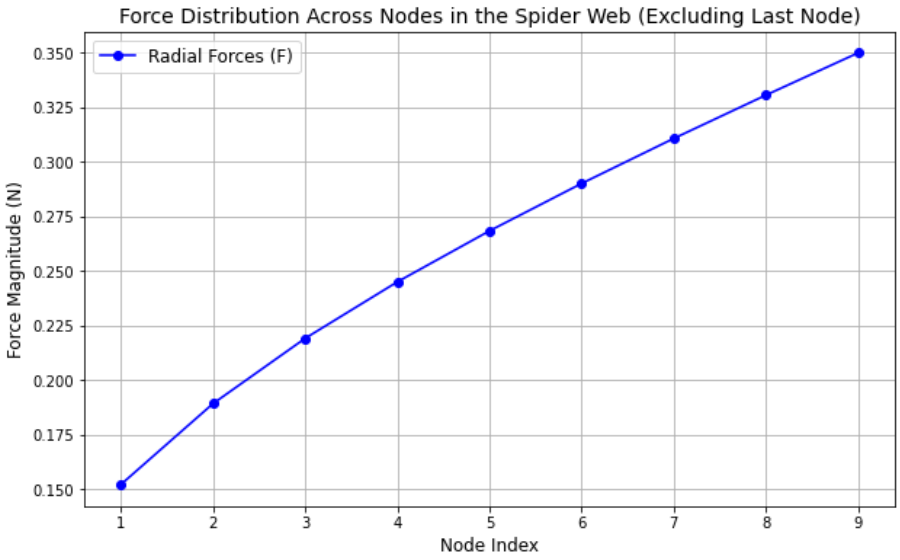

Figure 3.3: Force distribution across nodes in a spider web structure, showing radial forces (F) as a function of node index. The x-axis represents the node index, where nodes are sequentially numbered along a radial thread from the center outward, excluding the last node. The y-axis represents the force magnitude (N) applied at each node. The increasing trend indicates a rise in radial forces as the distance from the web center increases. This distribution is consistent with theoretical models and aligns with reference literature on mechanical properties of spider web structures.

Following the force distribution computation, the spider orb-web structure is modeled as a network of connected nodes, with the starting node indicated in green. Although this initial simulation reproduces the reference study's force distribution patterns, questions arise regarding the choice of the starting. These questions are addressed in later models.

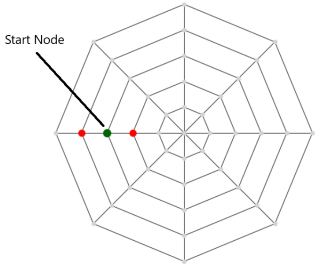

Figure 3.4: Spanned network structure in python environmet that mimic natural spider web.Indicating start node which can be chosen randomly.

Stage 2: Propagation

In the second stage, the model introduces signal propagation. The signal is treated as a traveling wave with a defined velocity that depends on the properties of the threads, such as tension and density. The simulation progresses iteratively, with each step representing a discrete time interval during which the signal moves to neighboring nodes. The algorithm ensures that the signal cannot revisit previously reached nodes in the same iteration, effectively preventing loops. At each step, the model updates the arrival time at each node and keeps track of the signal's path. This setup mimics the process of a wave propagating through the web and allows for initial studies of signal behavior under idealized conditions. To comprehensively assess the effectiveness of signal propagation models baseline performance metrics must be evaluated. These metrics include:

- Propagation Speed The rate at which signals traverse the network, measured as the time taken for a signal to travel from the source to various nodes.
- Amplitude Retention: The ability of the network to maintain signal strength over distance. This is quantified by comparing the amplitude of the signal at different points relative to its original strength.
- Collision Frequency (Interference Points): The number of points within the network where signals intersect, leading to potential interference. This metric helps identify areas of high signal congestion.

These metrics will be measured and compared across different lattice types, including traditional lattice networks and spider web-like structures.

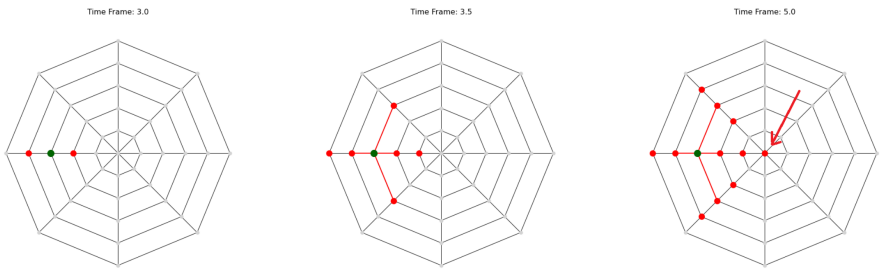

Figure 3.5: At time frames it can be seen that signal reaches nodes that are closer to initial node faster than nodes positioned father away.

Stage 3: Advanced Signal Propagation Model

In the third stage, the model is expanded to include a more complex network and refined signal propagation mechanisms. The signal is now capable of reaching a greater number of nodes, and additional parameters such as thread length and material properties are incorporated.

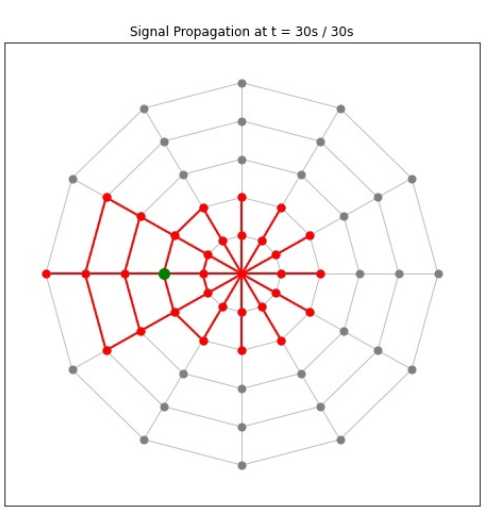

(a) Numerical model: Signal propagation is represented by nodes visited at discrete intervals. This model highlights general signal pathways but lacks precision in capturing continuous dynamics or collisions.

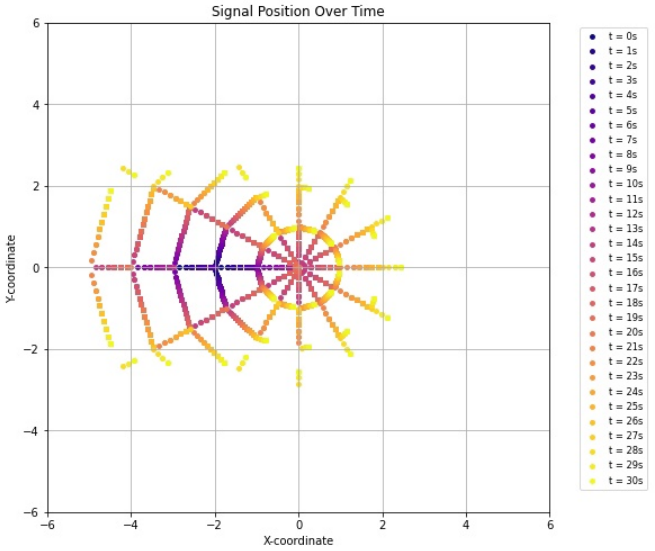

(b) Refined model: Continuous signal tracking reveals detailed propagation dynamics and identifies collision points where signals converge and interact.

Figure 3.6: Comparison of signal propagation models: (a) shows the discrete numerical model, while (b) illustrates the continuous refined model.

The two models presented for analyzing signal propagation in spider web-like structures demonstrate distinct levels of precision and insights. The first model, visualized in Figure 3.5a, calculates the nodes visited by the signal at discrete intervals. This approach captures the overall pathway and structure of the signal propagation but lacks the resolution to measure the signal's continuous behavior or its interactions between nodes. It provides a simpler representation of the propagation process, useful for identifying general patterns and connectivity in the network.

In contrast, the refined model, shown in Figure 3.5b, continuously tracks the signal's movement through the web over time. This model provides a more accurate and dynamic representation of signal propagation by incorporating details such as the timing and velocity of the signal's progression along the threads. Furthermore, it highlights instances where signals collide—points where multiple signal paths converge, potentially resulting in interference. The continuous tracking not only improves the spatial and temporal resolution of the propagation analysis but also allows for more precise identification of collision points and their effects on the overall signal behavior. Moreover, the model accounts for variations in the width and stiffness of connecting threads. Radial threads are typically stiffer and transmit signals faster than spiral threads, introducing a preferential radial movement of the signal. The magnitude of the signal is calculated using the formula:

$$|v| = \sqrt{\frac{F_t}{\mu}}$$

where F_t is the tension in the thread and μ is the mass per unit length. These parameters allow the model to simulate realistic signal dynamics, closely mirroring the physical properties observed in natural spider webs. By incorporating this level of detail, the model provides insights into how material properties and web geometry affect signal propagation and stability.

The comparison between the two models underscores the advantages of the refined approach. While the first model offers simplicity and ease of computation, the second model delivers enhanced accuracy and a deeper understanding of propagation dynamics, including critical phenomena like signal

collisions. These insights are invaluable for applications requiring detailed assessments of signal stability, efficiency, and potential interference in network structures.

3.3. Notes on Physics and Challenges of the Structure Model

Thickness, Materials, and Propagation Velocity

In spider orb webs, the structural differentiation between radial and spiral threads plays a crucial role in their mechanical properties and signal transmission capabilities. Radial threads, which serve as the primary framework of the web, are generally thicker and composed of stiffer silk compared to the more flexible spiral threads. Scanning electron microscopy (SEM) studies have measured the diameters of radial threads to range from approximately 2.67 to 5 micrometers, while spiral threads are thinner, with diameters between 0.72 and 1.04 micrometers. (Cranford et al., 2012)[10](ResearchGate: SEM Micrographs of Spider Web Components)[11] .

The velocity of signal propagation depends on the thread's stiffness and density. Radial threads, due to their rigidity and greater mass per unit length, facilitate faster transmission of mechanical vibrations. Research suggests that radial threads can transmit signals at speeds ranging from 50 to 70 m/s, while the more flexible spiral threads transmit signals at lower velocities, often in the range of 10 to 30 m/s (Sensenig et al., 2010)[12].

These velocity distinctions are critical for understanding how the spider web's dual-thread system balances rapid detection and energy dissipation. In research, this structural and functional differentiation is simplified to just fixed values and used as a model to study how varying material properties influence signal dynamics in complex networks.

In spider orb webs, the structural differentiation between radial and spiral threads plays a crucial role in their mechanical properties and signal transmission capabilities. Radial threads, which serve as the primary framework of the web, are generally thicker and composed of stiffer silk compared to the more flexible spiral threads (Mortimer et al., 2014)[13].

These velocity distinctions are critical for understanding how the spider web's dual-thread system balances rapid detection and energy dissipation. In research, this structural and functional differentiation is simplified to fixed values and used as a model to study how varying material properties influence signal dynamics in complex networks.

Specifically key metrics are,

- Signal Stability: Understanding how differences in propagation velocity affect the web's ability to maintain signal integrity across its structure.
- Collision Dynamics: Investigating how signals traveling at different velocities interact when they converge at nodes, potentially leading to interference.
- Network Optimization: Exploring how a combination of "fast" and "slow" threads in engineered networks can enhance robustness, reduce signal loss, and increase efficiency.

By incorporating the material and velocity distinctions of radial and spiral threads into numerical models, this contributes to the broader understanding of signal transmission dynamics in natural and artificial networks and research question.

Challenges in Collision Computation

The most recent model aimed to trace the exact paths of signals through the web structure. While theoretically robust, the computational complexity grew exponentially with the number of nodes and potential collision points. This model's fine-grained resolution, although detailed, resulted in prohibitively long simulation times, limiting its practicality for extensive studies. To address these computational challenges, three alternative methods were developed to balance accuracy and efficiency in collision detection: The first method involves a simplified model that follows the signal path with reduced resolution. This model tracks signal trajectories using a coarse grid, identifying collision points where paths intersect. While less precise, this approach significantly reduces computation time, making it suitable for preliminary analyses or scenarios where high accuracy is not critical. The second method employs a stochastic approach, simulating 1,000 signals that follow random paths through the web. Collisions

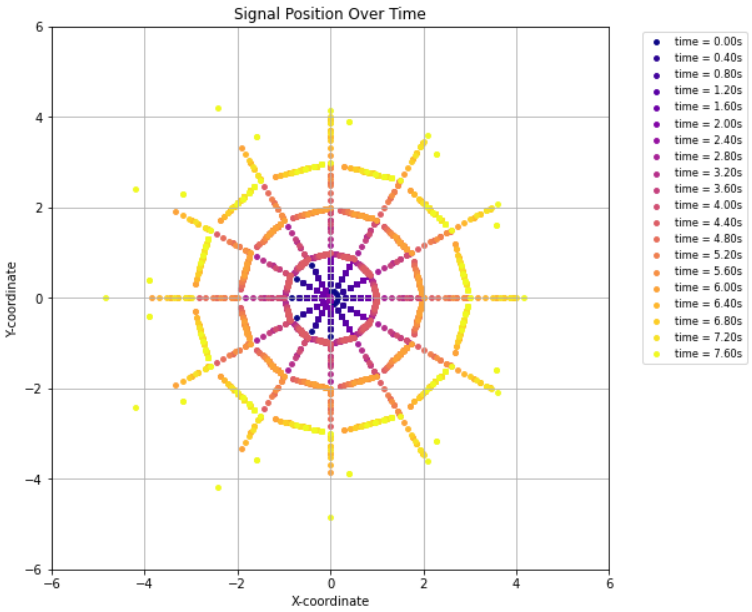

Figure 3.7: The graph illustrates the temporal propagation of a signal within a spider web-like network. Beginning at the central node (0,0), the signal traverses the edges, spreading outward along both radial (spoke) and spiral (ring) connections to analyze its transmission speed. The denser clusters of points near the center indicate slower radial propagation, while the outer arcs highlight the faster spiral spread.

are recorded when paths intersect. This model introduces randomness to account for variability in signal propagation but raises questions about the statistical robustness of the results. Future research should investigate whether increasing the number of signals to 100,000 would provide more reliable data and better symmetry in the collision patterns. The third and most computationally efficient method models signal propagation as a diffusion process. Signals are treated as wavefronts or packages that spread through the web structure. When wavefronts intersect, new packages are generated to simulate the resulting collisions. This approach leverages principles from diffusion theory to approximate signal behavior, offering a balance between computational speed and model accuracy. It shows promising potential for large-scale simulations due to its scalability and efficiency.

Each method presents unique advantages and limitations. The simple model offers speed at the expense of detail, the random walk model introduces variability but requires further validation, and the diffusion model provides an efficient yet reasonably accurate framework for studying signal collisions. Future work will focus on refining third models. Increasing the number of simulated signals and exploring alternative diffusion algorithms could enhance model accuracy. .

4

Methodology of the Propogation Models

This chapter explores different methods for modeling signal propagation and collisions in a spider web-like network. The simple collision approach analyzes how signals move through radial and spiral threads with different velocities, revealing that central nodes experience the highest activity and collision rates. Visualizations, including heatmaps and bar charts, demonstrate how network geometry influences signal dynamics.

To improve computational efficiency, a random walk method was introduced, simulating signals taking random paths. This method efficiently identifies collision-prone regions but lacks the accuracy of real-world wave propagation models. By applying this technique to different web structures, such as spiral and radial networks, distinct collision patterns emerge.

A more detailed wavefronts simulation refines signal propagation by introducing energy loss, adaptive transmission, and statistical analyses of signal paths and collisions. Compared to the random walk approach, this structured model provides deeper insights into network congestion and signal interference, though it requires greater computational resources. The results indicate that network topology strongly affects signal dispersion, with central nodes acting as key congestion points.

4.1. Simple Collision Approach

The model incorporates radial and spiral threads with distinct velocities, allowing study of node activity and collision frequencies. It uses the approach given in Chapter 3. The primary goal is to understand how signal distribution and interactions are influenced by the network's geometric configuration. Radial and spiral threads were assigned different lengths and propagation velocities to simulate real-world variances in signal transmission:

- Radial Threads: Constant length of 1 unit, with a velocity of 0.8 units/time.
- Spiral Threads: Are longer as $2\pi * sin(a)$, (where a in angle) with a velocity of 1.0 units/time.

Signals were propagated from the start node through the network using a priority queue to manage time-based events. Each signal's phase was calculated based on its path length and wavelength. Collisions were detected when signals arrived at the same node within a small error marge (1e-3 units). Three primary datasets were generated: the total number of times each node was visited by any signal,the number of collisions detected at each node, detailed paths and arrival times of individual signals.

The node activity heatmap (Figure 4.1ab) reveals that the central node (0, 0) experienced the highest activity, with 241 visits. Nodes closer to the center generally had higher visit counts due to the convergence of multiple signal paths. Collisions were most frequent at the network's center, aligning with the high node activity. The heatmap shows a gradual decrease in collision frequency as the distance from the center increases.

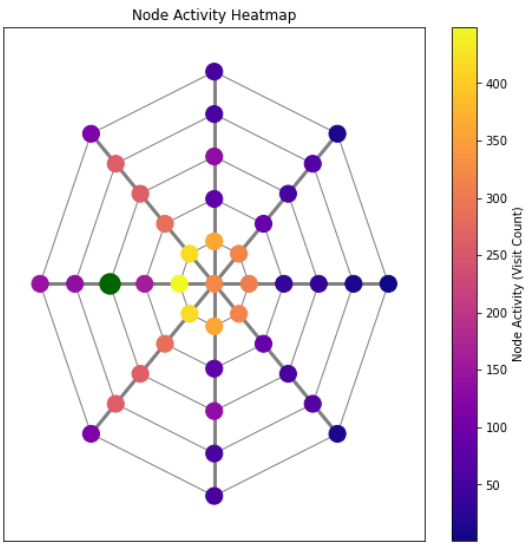

(a) The heatmap displays node visit frequencies. The initial node is shown green. The central node and nearby nodes are highlighted with brighter colors, indicating higher activity.

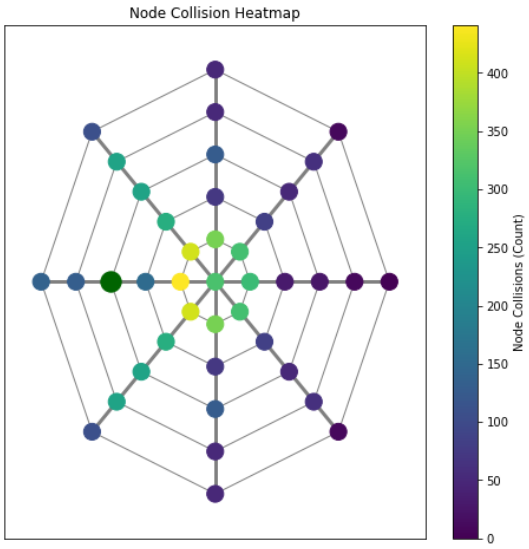

(b) Using a heatmap, the collision heatmap illustrates the frequency of signal collisions at each node. The central node shows the highest collision rate.

The simplified collision model demonstrates the dynamics of signal propagation and collision in a spider web-like network. The center node experiences the highest activity and collision rates due to signal convergence. Radial threads, with slower velocities, contribute to higher collision probabilities near the center. Outer nodes exhibit fewer visits and collisions, highlighting the impact of network geometry on signal dynamics. Centered aligned node in a network experience more visits and collisions due to their structural and functional roles. They tend to have higher connectivity, serving as hubs that link multiple nodes together. This makes them part of the shortest or most efficient paths, causing signals to frequently pass through them. As multiple signals converge at these nodes, the likelihood of collisions increases, especially in systems where simultaneous data transmission occurs. Additionally, central nodes often act as bottlenecks or critical points in the network, concentrating traffic flow and further raising the chances of revisits and collisions. In spider web-like structures, these nodes might correspond to intersections of radial and spiral threads, becoming focal points for signal propagation and interference.

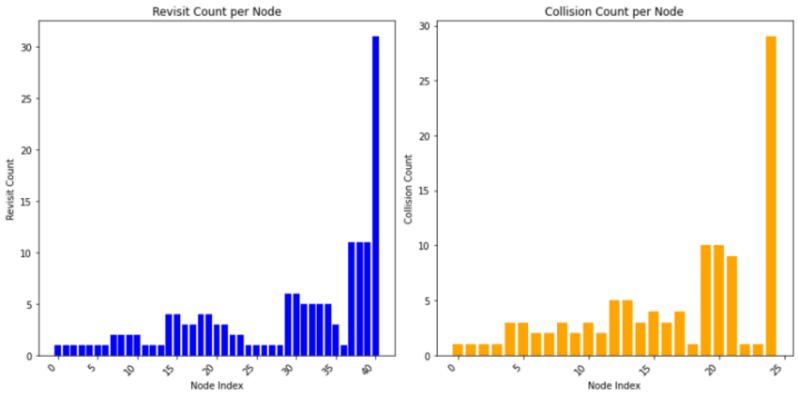

Figure 4.2: Two bar charts illustrate the distribution of revisit and collision counts per node. Lower indices correspond to nodes near the center of the web, higher indicesrepresent nodes closer to the outer edges of the web. The left chart shows that most nodes have low revisit counts, except for a sharp spike at the highest node index, exceeding 30 revisits. Similarly, the right chart reveals a generally low collision count, with a significant peak near the highest node index, reaching nearly 30 collisions.

4.2. Random Walk Study

To avoid heavy computations method of random walk was implemented. The simulation approach involves randomly assigning an initial direction to a predefined number of signals, all starting from the same point. These signals propagate along the structure's predefined pathways, following the geometric constraints of the web. Ideally it should simulate one signal path moving along the web. If two or more signals reach the same location at the same time, a collision is recorded. The final step is to visualize these collisions to analyze the network's efficiency and propagation characteristics. To illustrate the method, a graph (Figure 4.3) was created to represent the propagation of three distinct signals. This basic representation serves as a proof of concept to demonstrate how signals travel within the web and how collisions occur. Final structure shows likely accurate signal reach.

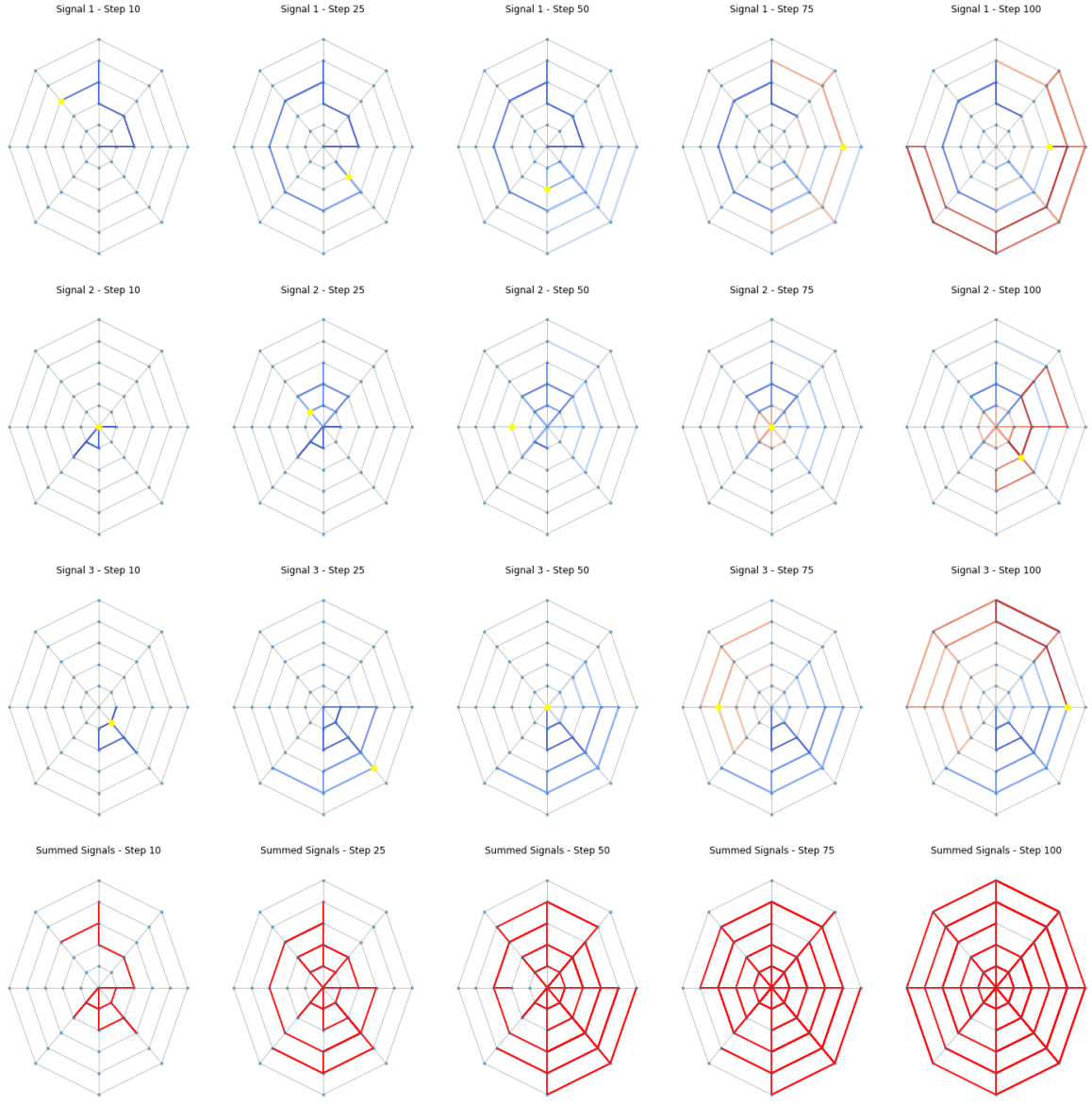

Figure 4.3: The following image presents a series of snapshots showing signal propagation and collisions over time in a spider web lattice. The top three rows illustrate individual signals moving through the structure, while the bottom row shows the cumulative effect of multiple signals interacting. The intensity of the red lines in the final frames highlights regions with higher collision frequencies and coverege of the web.

Mathematical Model Description

Edges are added in three categories:

1. **Vertical (Radial) Edges:** Connect nodes along the same arm:

$$\{(a, \ell), (a, \ell + 1)\} \quad \text{for } \ell = 0, 1, \ldots, L - 2.$$

2. **Circular (Neighbor) Edges:** Connect nodes at the same level in adjacent arms:

$$\{(a, \ell), ((a + 1 \mod A), \ell)\} \quad \text{for each } a \text{ and } \ell.$$

3. **Diagonal Edges:** Connect nodes from one arm and level to the adjacent arm and the next level:

$$\{(a, \ell), ((a + 1 \mod A), \ell + 1)\} \quad \text{for } \ell = 0, 1, \ldots, L - 2.$$

Random Walk and Collision Simulation

A signal starts at a chosen start node i_0 and performs a random walk over the graph. Let the signal's position at step t be i_t. The dynamics are as follows:

1. **Transition Rule:** At each step t, the signal moves from node i_t to a neighbor chosen uniformly at random:

$$i_{t+1} \sim \text{Uniform}\{j \in \mathcal{N}(i_t)\},$$

where $\mathcal{N}(i_t)$ is the set of neighbors of node i_t.

2. **Collision Event:** When traversing an edge $e = (i_t, i_{t+1})$, a collision can occur with another signal reaching same time t. Another signal should reach same node or same edge at the same time, multiple collisions possible. Records are noted in a list. Simulation follows time Tevalutaions for all randomwalks. If a collision occurs, record the midpoint of the edge or node:

$$\mathbf{m}_e = \frac{1}{2}\Big(\mathbf{p}(i_t) + \mathbf{p}(i_{t+1})\Big),$$

where $\mathbf{p}(i) = (x(i), y(i))$ is the position of node i.

3. **Simulation Parameters:** Let:

$$N_{\text{signals}} : \text{total number of signals}, \quad T : \text{number of steps per signal}.$$

The total number of steps simulated is $N_{\text{signals}} \times T$.

The second and third images (Figures 4.4a, 4.4b) provide insight into how this method can be applied beyond traditional web structures. Instead of a standard lattice, the simulation was performed on more complex web-like geometries. In the Spiral Web, signals propagate along a spiraling network of nodes. Due to its configuration, collisions appear concentrated in the central regions, where paths are denser. In the Traditional Spider Web, signals move along radial and circumferential paths, producing a different collision pattern. The intersections occur mostly near the central hub and along key connecting points where multiple pathways converge. By analyzing these visual outputs, we can infer how different structures impact signal dispersion and collision distribution.

While this method provides an interesting way to analyze signal behavior, it is unclear whether it accurately models real-world propagation. Several factors must be investigated to determine its validity. The assumptions made in the simulation (such as random signal direction and discrete time steps) may not fully align with how waves propagate. In reality, signals may experience attenuation, diffraction, or interference that is not accounted for in the current model. The results may change significantly with a larger number of signals or different web configurations, requiring further simulations to determine patterns at larger scales.

One significant difficulty in this approach is the computational power to proof if its indeed good simulation of real signal propagation. To calculate real signal in this structure is difficult. Simulating signals over complex structure with time steps demands substantial processing resources. As the complexity of the web structure increases, the computational load grows exponentially, making it challenging to

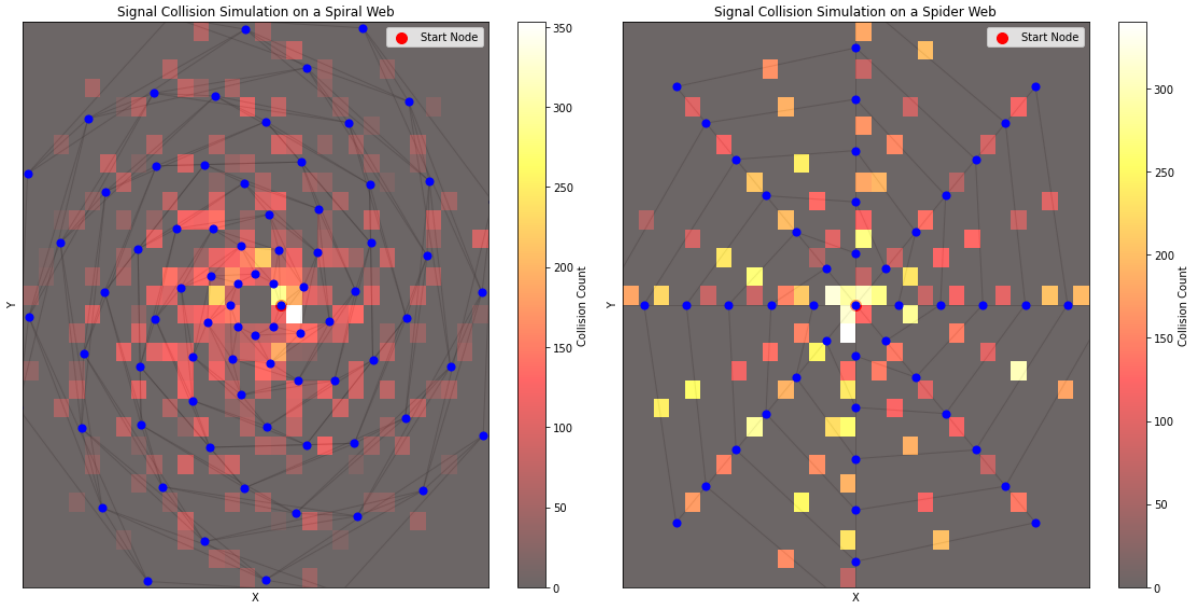

(a) The spiral web (a) follows a continuous, curved pattern where nodes are connected more fluidly.Number signals $= 500$, number steps $= 100$. The highest collision density occurs near the center, but the distribution is diffused, gradually decreasing outward. This structure disperses signal traffic more evenly, reducing abrupt congestion points and creating a smoother but broader collision spread.

(b) In the radial spider web (b), the structure consists of straight spokes connected by concentric circular threads. Number signals $= 500$, number steps $= 100$. The highest collision density is observed at the center, where multiple signal paths converge. While this design efficiently directs signals, it also creates abrupt congestion points due to sharp directional changes at nodes.

scale simulations for highly detailed models. Despite these uncertainties, if a sufficient number of signals are simulated with realistic propagation parameters, this approach could offer meaningful insights into wave dynamics in network-like structures. By refining the model potentially incorporating signal loss, varying propagation speeds, or environmental effects this method might become a more accurate representation of real world signal behavior. However, limitations remain in terms of computational feasibility, accuracy, and the ability to generalize results to different systems. Future studies should focus on improving the physical basis of the simulation and validating it against empirical data.

4.3. Wavefronts Simulation

To simulate propagation, a discrete time-step model is used, where each node forwards the signal to its neighbors. If multiple signal packets reach a node simultaneously, they merge, their combined intensity reduces based on an energy loss factor, and travel histories are recorded. Energy loss is introduced to mimic real-world attenuation effects. The model captures different aspects of propagation, including collision detection, intensity decay, path tracking, and network saturation. Various parameter tuning techniques were implemented to test how different network configurations influence signal behavior. An adaptive weighting mechanism dynamically adjusts transmission strength based on past collision data, allowing for a more realistic simulation of real-world adaptive networks.

Mathematical Model of Signal Propagation Wavefront

A *packet* p is characterized by:

- Its current edge: $(i, j) \in E$,
- A normalized *position* $x \in [0, 1]$, where $x = 0$ corresponds to node i and $x = 1$ corresponds to node j,
- An *intensity* I,
- A *collision count* C,
- A *path* $\mathcal{P} = [i_0, i_1, \ldots, i_k]$ recording the nodes visited,
- A current *time* t.

Packet Propagation

The propagation occurs in discrete time steps of size Δt. A packet on edge (i, j) updates its position according to:

$$x(t + \Delta t) = x(t) + \frac{v\,\Delta t}{L_{ij}},$$

where v is the constant signal velocity. When the packet reaches the end of the edge (i.e. when $x \geq 1$), it is considered to have arrived at node j.

Spawning New Packets

Upon arrival at node j at time t_{arrival}, new packets are spawned along each outgoing edge from j, except for the edge leading back to the previous node in the packet's path. Each spawned packet p' is initialized with:

$$x_{p'}(t_{\text{arrival}}) = 0, \quad I_{p'} = I_p, \quad C_{p'} = C_p, \quad \mathcal{P}_{p'} = \mathcal{P}_p \cup \{j\}.$$

Collision Detection and Merging

Consider packets p and q traveling along the same edge (i, j) with positions x_p and x_q, respectively. A collision is detected if

$$|x_p - x_q| < \epsilon,$$

where ϵ is the collision threshold. When packets collide, they merge to form a new packet p_{merged} with the following properties:

$$\begin{aligned}
\text{Position:} \quad & x_{\text{merged}} = \frac{x_p + x_q}{2}, \\
\text{Intensity:} \quad & I_{\text{merged}} = \eta\,(I_p + I_q), \\
\text{Collision count:} \quad & C_{\text{merged}} = \max(C_p, C_q) + 1, \\
\text{Time:} \quad & t_{\text{merged}} = \max(t_p, t_q),
\end{aligned}$$

with η being the *fade factor* (e.g., $\eta = 1$ means no fading).

If a packet's collision count reaches a prescribed maximum C_{max}, the packet is removed from the simulation.

Summary of the Simulation Steps

1. **Initialization:**
   - Build the spider-web graph with nodes arranged in concentric layers.
   - Place the initial signal packet(s) at the start node (or along its adjacent edges).
2. **Propagation:** For each packet on edge (i, j):

$$x \leftarrow x + \frac{v\,\Delta t}{L_{ij}}.$$

3. **Arrival:** If $x \geq 1$, record the arrival at node j and spawn new packets along outgoing edges from j (excluding backtracking).
4. **Collision Detection:**
   - Group packets by the edge on which they travel.
   - For each group, if any pair satisfies $|x_p - x_q| < \epsilon$, merge them as described above.
5. **Termination:**
   - The simulation stops at a maximum time T_{max} or when no packets remain.
   - Additional statistics (arrival times, path lengths, collision counts, etc.) are recorded.

Results

While the model provides valuable insights, it has several limitations. Although adaptive weighting is included, full dynamic rerouting of signals is not implemented, which could further enhance accuracy. The decay function is a simple factor rather than a complex, environment-dependent function, and the study does not account for noise or other interfering signals that could impact real-world network efficiency. The results are summarized in the following statistics.

Compared to a random walk, the structured propagation in this model ensures controlled signal movement and provides clearer patterns of collision formation. While the alternative method offers a more computationally efficient way to analyze collisions by simplifying signal initiation, it lacks the ability to represent attenuation, diffraction, and interference effects accurately. The random assignment of initial signal paths in the alternative model may lead to inconsistencies in propagation results. Additionally, the alternative model only captures a snapshot of possible propagation paths rather than a fully evolving network state, limiting its predictive capabilities. While the structured model in this project requires greater computational power, it offers a more detailed view of how collisions evolve over time, allowing for better insights into optimizing network designs. The structured model also incorporates energy dissipation and collision intensity analysis, which are absent in the alternative approach. This makes the structured model a better choice for applications requiring precise modeling of signal behavior, such as biological signal transmission, wireless communication networks, and material stress analysis. However, the alternative method may still be useful in rapid preliminary assessments where computational efficiency is a priority.

The resolution of the heatmap (Figure 4.6) can be improved with greater computational resources. Higher grid precision and finer resolution will allow a more detailed representation of collision intensity and better identification of congestion points. With enhanced computational capacity, more nodes can be analyzed simultaneously, leading to a more refined understanding of interference zones and potential weak points in the structure.

The heatmap also reflects how signal dispersion is influenced by the interplay of radial and spiral connections, with some areas experiencing more frequent interactions than others. These insights could be beneficial in optimizing network design to minimize signal loss and improve overall transmission efficiency. To enhance the model, several improvements can be made in future work. Incorporating machine learning would allow predictive modeling so the network can adapt its transmission paths based on previous collision data. Adding stochastic elements by introducing randomness in propagation speed and energy decay could better simulate real-world uncertainties.

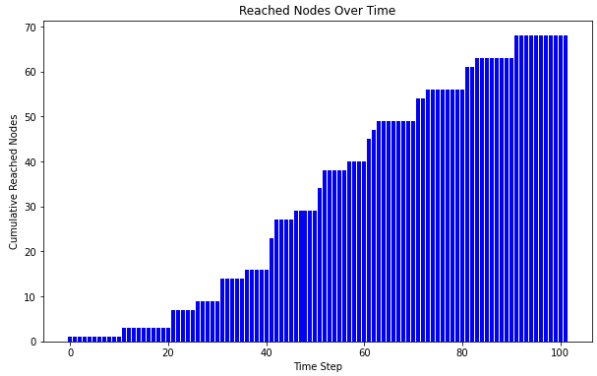

(a) This plot represents the number of signal collisions occurring at each time step. Initially, few collisions take place as the signal is still dispersing. However, as the signal spreads through the network and different paths begin to overlap, the number of collisions rises. The fluctuations in the latter half of the timeline show how interference changes dynamically.

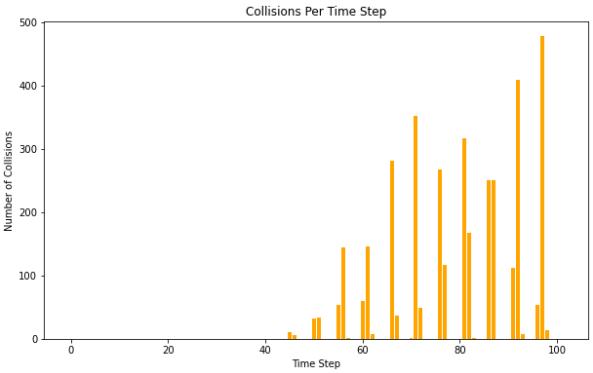

(b) This histogram captures the distribution of path lengths taken by individual signal packets. The peak in the middle indicates that most signals travel a moderate number of steps before either merging in a collision or fading due to energy loss. The presence of shorter and longer paths demonstrates variation in network topology and travel efficiency.

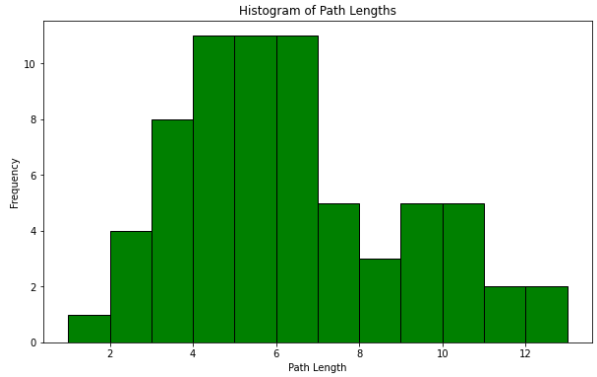

(c) This plot shows the cumulative number of nodes that have been reached by the signal over time. Initially, growth is slow as the signal starts its journey. Once more paths open, the number of influenced nodes increases rapidly, eventually plateauing as the signal has reached all accessible points in the network.

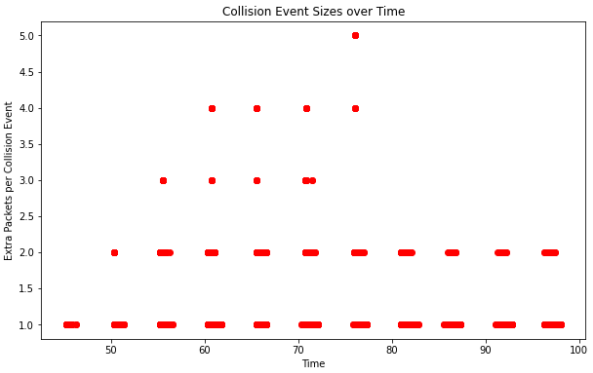

(d) This scatter plot shows the size of each collision event over time, measured by the number of extra packets merging per event. Early on, small collisions dominate since only a few signal paths overlap. As the signal spreads, large collision events become more common, peaking in intensity before tapering off as paths become fully merged or signal energy fades.

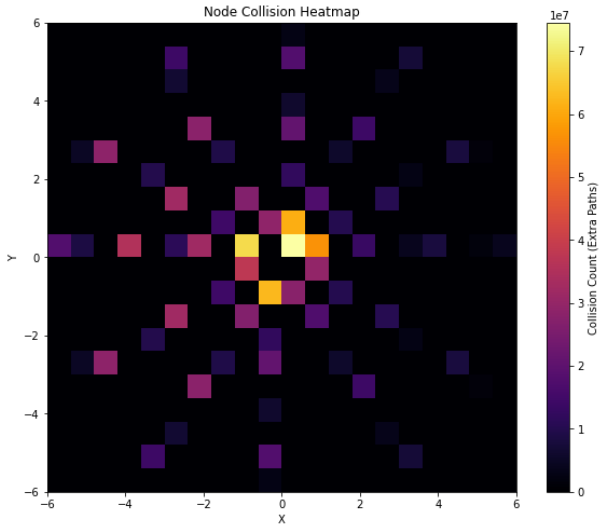

Figure 4.6: This heatmap visualizes the density of signal collisions throughout the network. Start node (3,6) left. The central nodes experience the highest number of collisions due to the convergence of multiple signal paths, while the intensity decreases outward as signals dissipate.

5

Advanced Model and Defected Model

5.1. Introducing Advanced Forces Model

Let the web be modeled as a mass–spring network with N nodes. Each node has a position

$$\mathbf{x}_i(t) = \begin{pmatrix} x_i(t) \\ y_i(t) \end{pmatrix}, \quad i = 0, \ldots, N-1,$$

with equilibrium positions $\mathbf{x}_i^0$. In our construction, the central node is

$$\mathbf{x}_0^0 = (0, 0),$$

and the remaining nodes are placed on concentric rings. The nodes on each ring are evenly spaced with angles

$$\theta = \frac{2\pi j}{N_{\text{radials}}}, \quad j = 0, 1, \ldots, N_{\text{radials}} - 1,$$

and with radial distances proportional to the ring index.

The network's connectivity is given by a set of edges. Each edge connecting nodes i and j is assigned a rest length

$$L_{ij} = \|\mathbf{x}_i^0 - \mathbf{x}_j^0\|.$$

For nodes connected by a spring, the force is computed by Hooke's law:

$$\mathbf{F}_{ij} = -k\Big(\|\mathbf{x}_i - \mathbf{x}_j\| - L_{ij}\Big)\frac{\mathbf{x}_i - \mathbf{x}_j}{\|\mathbf{x}_i - \mathbf{x}_j\|}.$$

The total force on node i is then the sum over all its neighbors:

$$m\,\ddot{\mathbf{x}}_i = \sum_{j \in \mathcal{N}(i)} \mathbf{F}_{ij} - c\,\dot{\mathbf{x}}_i - k_r\left(\mathbf{x}_i - \mathbf{x}_i^0\right),$$

where

- m is the mass per node,
- c is the viscous damping coefficient,
- k_r is a weak ground (restoring) spring constant that forces free nodes back toward equilibrium,
- For fixed nodes (e.g. on the outermost ring) we impose $\mathbf{x}_i(t) = \mathbf{x}_i^0$ for all t.

The system is cast in first order form by defining the state vector

$$\mathbf{y}(t) = \begin{pmatrix} \mathbf{x}_1(t) \\ \vdots \\ \mathbf{x}_N(t) \\ \dot{\mathbf{x}}_1(t) \\ \vdots \\ \dot{\mathbf{x}}_N(t) \end{pmatrix} \in \mathbb{R}^{2N}.$$

Thus, the equations of motion become

$$\frac{d}{dt}\mathbf{y}(t) = \begin{pmatrix} \dot{\mathbf{x}}(t) \\ \frac{1}{m}\left[\sum_{j\in\mathcal{N}(i)} -k\Big(\|\mathbf{x}_i - \mathbf{x}_j\| - L_{ij}\Big)\frac{\mathbf{x}_i - \mathbf{x}_j}{\|\mathbf{x}_i - \mathbf{x}_j\|} - c\,\dot{\mathbf{x}}_i - k_r\left(\mathbf{x}_i - \mathbf{x}_i^0\right)\right] \end{pmatrix}.$$

For fixed nodes the derivatives are forced to zero.

The numerical integration is performed using a Runge-Kutta method (via `solve_ivp`) with tight tolerances (e.g., $rtol = 10^{-9}$ and $atol = 10^{-12}$) over a time interval $t \in [0, 20]$ seconds with 401 time steps.

The total energy of the system is computed at each time step as

$$E(t) = \frac{1}{2}m\sum_{i=0}^{N-1}\|\dot{\mathbf{x}}_i(t)\|^2 + \frac{1}{2}k\sum_{\langle i,j\rangle}\Big(\|\mathbf{x}_i(t) - \mathbf{x}_j(t)\| - L_{ij}\Big)^2.$$

A specific node (e.g. node with index 10) is given an initial velocity pulse

$$\dot{\mathbf{x}}_{10}(0) = \text{pulse\_strength} \times \begin{pmatrix} 0 \\ 1 \end{pmatrix},$$

and its displacement relative to equilibrium,

$$\Delta_{10}(t) = \|\mathbf{x}_{10}(t) - \mathbf{x}_{10}^0\|,$$

is monitored.

The Fast Fourier Transform (FFT) is applied to the time series of the pulsed node's displacement in order to reveal its frequency content. Denote by

$$d(t) = \left\|\mathbf{x}_{\text{pulsed}}(t) - \mathbf{x}_{\text{pulsed}}^0\right\|$$

the displacement magnitude of the pulsed node, where $\mathbf{x}_{\text{pulsed}}^0$ is its equilibrium position. In the simulation, a discrete set of measurements $d(t_n)$ is obtained over the time interval $t \in [0, T]$.

Before applying the FFT, the mean value is subtracted :

$$d'(t_n) = d(t_n) - \langle d(t)\rangle,$$

where

$$\langle d(t)\rangle = \frac{1}{N}\sum_{n=0}^{N-1} d(t_n).$$

The FFT is then computed using

$$\hat{d}(f_k) = \sum_{n=0}^{N-1} d'(t_n)\, e^{-2\pi i f_k t_n},$$

where f_k are the discrete frequency bins. In Python code, this is implemented with the function `fft` from the `numpy.fft` module, and the corresponding frequency bins are generated using `fftfreq`.

Plotting the amplitude spectrum $|\hat{d}(f)|$ versus frequency f provides insight into the dominant oscillation modes of the network. Peaks in this spectrum correspond to the natural frequencies of the system. This analysis is particularly useful for understanding the effects of damping and the nonlinear behavior of the spring–mass system, as the spectral content may shift or broaden compared to the predictions of a purely linear model.

The model implements these ideas as follows:

1. The nodes are generated and stored in an array. Edges are constructed between nodes according to the geometry.
2. The equations of motion are derived by summing the forces from each spring (using the nonlinear expression for the distance), adding viscous damping, and including the extra restoring force (only for free nodes).
3. The state vector $\mathbf{y}(t)$ is formed by concatenating positions and velocities.
4. The ODE system is solved numerically using `solve_ivp`.
5. Energy, displacement magnitude, and component displacements are computed for analysis.
6. Several graphs are produced:
    - 2D snapshots of the web at regular time intervals, colored by the x-displacement.
    - Time series plots of total energy and the displacement of the pulsed node.
    - FFT and spectrogram analyses of the pulsed node's displacement.
    - 3D deformation snapshots in which the horizontal coordinates remain fixed at their equilibrium values and the vertical coordinate shows $z_i(t) - z_i^0$

5.1.1. Resluts

A pulse is applied to a selected node, imparting an initial velocity in the upward direction. The system is solved numerically using the Runge-Kutta method implemented. Key simulation parameters include:

- Number of rings: 5
- Number of radial spokes: 8
- Mass per node: $m = 1.0$
- Spring constant: $k = 100.0$
- Damping coefficient: $c = 0.1$
- Ground restoring force: $k_r = 1.0$
- Pulse magnitude: 0.05 m/s

The simulation runs for 20 seconds with 401 time steps.

Figure 5.1 presents a series of 3D snapshots illustrating the temporal evolution of the web's deformation under an initial perturbation. The results indicate that the pulse propagates through the structure in a wave-like manner, with reflections occurring at the fixed boundary. As the wave traverses the web, the interactions between the periodic arrangement of masses and springs give rise to complex interference patterns, influencing the amplitude, phase, and duration of oscillations. The interplay between tensile forces in the radial threads and the elasticity of the spiral threads leads to local variations in wave speed, further contributing to the observed distortions in wavefronts.

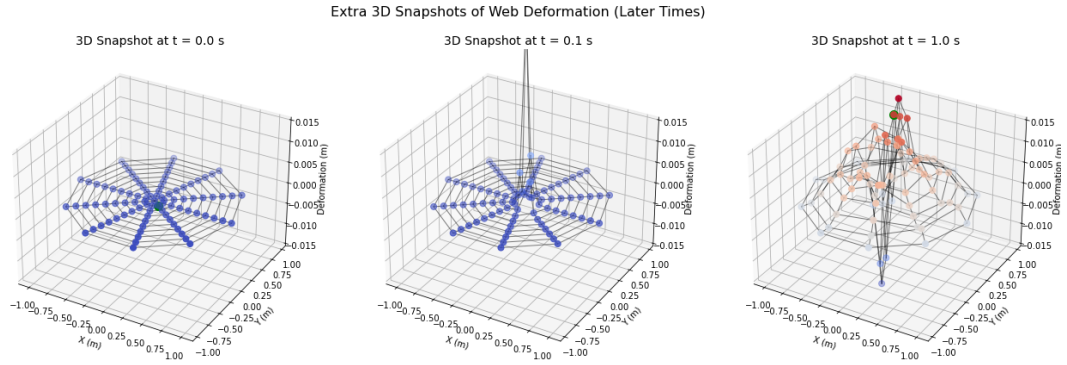

Figure 5.1: 3D snapshots of the web deformation at different time steps. The initial perturbation propagates outward and reflects from the fixed boundary, generating complex interference patterns.

The total energy of the system, calculated as the sum of kinetic and potential energies, decreases over time due to damping effects, as shown in Figure 5.2. The decay in energy follows an approximately exponential trend, suggesting that the damping mechanism effectively absorbs vibrational energy, preventing indefinite oscillations. This behavior aligns with the expected outcome of a dissipative system, where energy is continuously removed through internal friction and air resistance. The rate of decay is influenced by the damping coefficient, which determines how quickly the system reaches equilibrium. Notably, energy dissipation is more pronounced in regions where wave reflections are strongest, indicating that boundary interactions contribute significantly to energy loss.

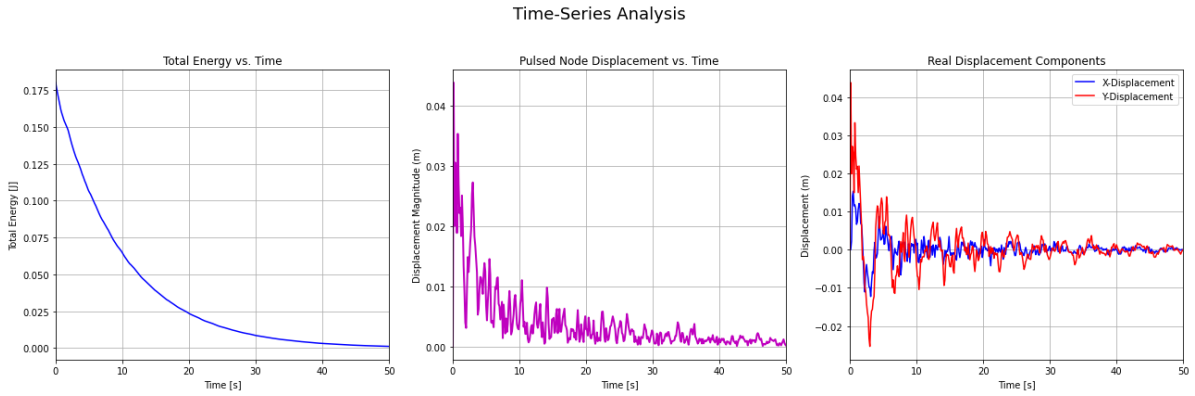

Figure 5.2: Total energy vs. time showing exponential decay due to damping. Average fluctuations nodes on graph. The energy dissipation rate depends on the damping coefficient and boundary interactions.

5.1.2. Displacement Analysis

The displacement of the initially perturbed node decreases progressively over time, as depicted in Figure 5.3. The oscillatory motion is gradually dampened, resulting in reduced displacement magnitude. This attenuation is a direct consequence of energy dissipation through damping and wave dispersion within the structure. The displacement response exhibits a characteristic decay pattern, consistent with a damped harmonic oscillator. Additionally, secondary oscillations induced by wave reflections modify the displacement trajectory, creating transient fluctuations before the system stabilizes.

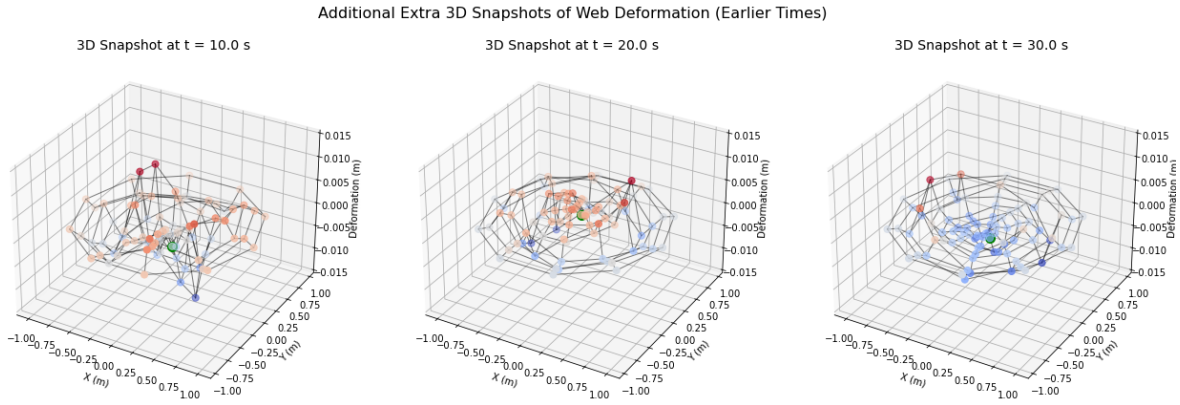

Figure 5.3: Time evolution of displacement magnitude of the pulsed node. The oscillations gradually decay due to energy loss, with transient fluctuations caused by wave reflections.

To further analyze the oscillatory behavior, a frequency-domain representation of the node displacement is obtained using a Fast Fourier Transform (FFT), as shown in Figure 5.4. The dominant frequency corresponds to the fundamental vibrational mode of the structure, while additional peaks indicate higher-order harmonics and interference-induced frequency components. The observed spectrum is consistent with that of a damped harmonic system, where the primary oscillation frequency remains prominent while higher-frequency components diminish over time. The reflections from the fixed boundary introduce spectral broadening effects, modifying the displacement characteristics in both the time and frequency domains.

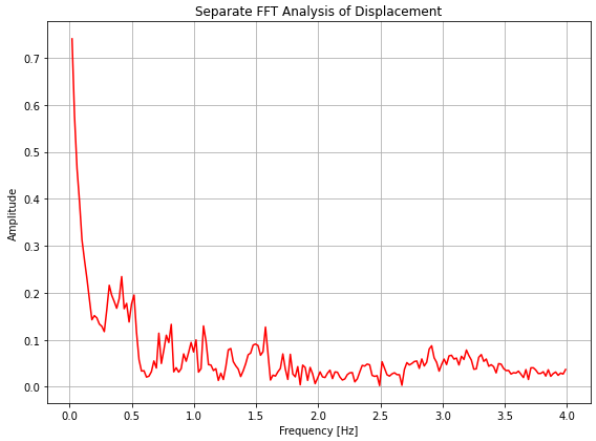

Figure 5.4: FFT analysis of the pulsed node displacement, highlighting dominant frequencies and spectral broadening effects.

The simulation results provide valuable insights into the wave propagation dynamics within a spider web-like structure. The interaction between mass-spring elements, boundary reflections, and damping effects governs the signal transmission efficiency in such networks. These findings have potential implications for understanding biological signal processing in natural spider webs, as well as for designing bio-inspired communication and sensing networks.

5.2. Defects Definition

5.2.1. Introducing Adjustment to Structure, Physical Consequences of Defects

In modeling a physical network, certain nodes may become inactive, meaning they are effectively removed from the system and do not contribute to the dynamics. To account for this phenomenon, we introduce a Boolean function $\mathbb{I}_{\text{active}}(i)$ which determines whether node i is active. The probability that a node is inactive is given by p_{missing}.

where $U_i \sim \text{Uniform}(0,1)$ is a uniformly distributed random variable. The presence of inactive nodes must be managed to ensure the structural integrity of the system. Special boundary conditions ensure that the central node (denoted as $i = 0$) and nodes in a predefined fixed set remain active:

$$\mathbb{I}_{\text{active}}(0) = 1, \quad \mathbb{I}_{\text{active}}(j) = 1 \text{ for } j \in S_{\text{fixed}}.$$

In many real-world networks, mass irregularities can arise due to physical imperfections or environmental influences. To simulate such irregularities, each node is assigned a mass m_i, which under ideal conditions is set to a uniform default value m_{default}. However, to incorporate variability, the mass of an active node may be perturbed by a random multiplicative factor. With probability p_{mass}, the new mass of node i is given by:

$$m_i = m_{\text{default}} \cdot \alpha_i, \quad \alpha_i \sim \text{Uniform}(\alpha_{\min}, \alpha_{\max}).$$

Only active nodes are subject to this transformation. The effect of these irregularities propagates through the system by influencing the forces acting on the nodes and their subsequent accelerations.

Each structural connection between two nodes (i, j) is associated with an equilibrium length L_0. However, defects in the network can compromise these connections in two primary ways. First, an edge may be entirely removed due to structural failure. The probability of an edge between two active nodes being removed is denoted p_{broken}, and the presence of an edge follows:

$$\mathbb{I}_{\text{edge}}(i,j) = \begin{cases} 0, & \text{if } U_{ij} < p_{\text{broken}}, \\ 1, & \text{otherwise}, \end{cases}$$

where $U_{ij} \sim \text{Uniform}(0,1)$ is independently sampled for each edge. The removal of an edge alters the connectivity of the system and may lead to fragmentation in extreme cases.

For edges that are not entirely removed, there remains the possibility of weakening. A weakened edge experiences a reduction in its stiffness coefficient, modifying its ability to transmit forces. This occurs with probability p_{weakened}, and the new stiffness is given by:

$$k_{\text{edge}} = \begin{cases} k_{\text{default}}, & \text{if the edge is not weakened}, \\ k_{\text{default}} \cdot f_{\text{weakened}}, & \text{otherwise}. \end{cases}$$

where f_{weakened} is a predefined reduction factor. The consequence of such modifications extends to the forces experienced by the nodes, fundamentally altering the system's response to external stimuli.

Nodes that become inactive do not undergo motion, and their velocity and acceleration satisfy:

$$\mathbf{v}_i = 0, \quad \mathbf{a}_i = 0.$$

For active nodes, the dynamics are governed by Newton's Second Law, where the acceleration is given by:

$$\mathbf{a}_i = \frac{\mathbf{F}_i}{m_i}.$$

The force exerted between two connected nodes is governed by Hooke's Law, which describes the restoring force due to an elastic connection. If an edge remains in the system, the force acting between two connected nodes i and j is given by:

$$\mathbf{F}_{ij} = -k_{\text{edge}} \left(\|\mathbf{r}_i - \mathbf{r}_j\| - L_0 \right) \frac{\mathbf{r}_i - \mathbf{r}_j}{\|\mathbf{r}_i - \mathbf{r}_j\|}.$$

Here, the stiffness coefficient k_{edge} may take different values depending on whether the edge has been weakened, leading to significant alterations in the behavior of the network under applied forces. These variations in connectivity, mass distribution, and force transmission collectively define the mechanical properties of the system and contribute to emergent behaviors observed in complex networks.

5.2.2. Results

Following the equations compared two configurations of a spider web model: an *Ideal Web* with uniform stiffness and connectivity, and a *Defective Web* in which certain nodes are missing and some edges are weakened. The following figures (5.5 5.6)illustrate the dynamic responses and provide insight into the underlying causes of the observed differences.

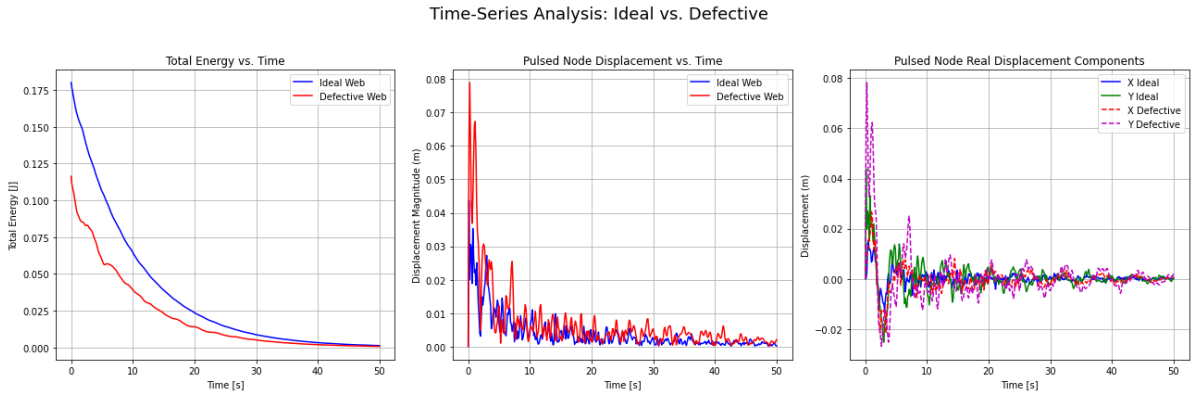

Figure 5.5: Grap represent time series of defected vs ideal web. Total Energy vs. Time (Left), Pulsed Node Displacement vs. Time (Center), Real Displacement Components (X, Y) (Right).

Both configurations show an overall decay in energy due to damping. However, the *Defective Web* exhibits a modified decay profile. The defects (missing nodes and weakened edges) disrupt the uniform stiffness and connectivity, leading to non-uniform energy transfer and dissipation. As a result, the pathway for energy to be stored and dissipated is altered, manifesting as deviations in the energy decay curve.

The displacement of the node receiving the initial pulse is similar in both cases at early times, but differences become more pronounced as time progresses. Initially, the local impact of the pulse dominates the response. Over time, however, the altered local stiffness and connectivity in the *Defective Web* modify its natural vibration modes and damping characteristics, leading to differences in oscillation amplitude and decay rates.

The decomposition into X- and Y-components reveals subtle phase shifts and amplitude variations in the *Defective Web* compared to the *Ideal Web*. The asymmetry introduced by defects causes imbalances in force transmission along different directions. This results in altered modal shapes and phase differences, evidencing the sensitivity of the dynamic response to local structural changes.

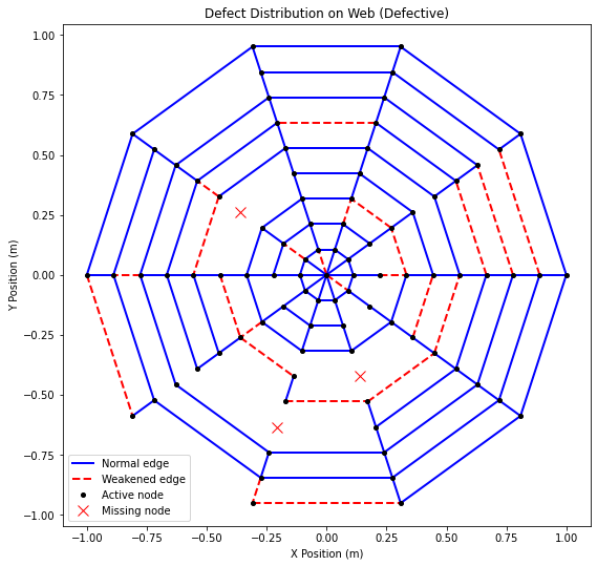

Figure 5.6: The diagram highlights several key modifications in the *Defective Web*: Normal edges (blue): These remain intact and maintain their full stiffness. Weakened edges (red dashed): These edges have reduced stiffness, compromising the overall structural integrity. Missing nodes (red X): Nodes are entirely removed, disrupting the continuity of the w .

The comparative analysis between the *Ideal* and *Defective* web models reveals that structural defects significantly influence the dynamic behavior:

- Energy Decay: The presence of defects alters the pathways for energy transfer and dissipation. In the *Defective Web*, the irregular stiffness and connectivity cause variations in how energy is stored and gradually dissipated over time.
- Displacement Response: Although the initial response to the pulse is similar, the lack of uniformity in the defective structure leads to divergent displacement behaviors. The natural frequencies and damping properties are locally modified, resulting in amplitude differences and phase shifts in the oscillatory response.
- Wave Propagation: The disrupted connectivity in the *Defective Web* affects how vibrational waves travel through the structure. This is evident in the spatial distribution of deformations and the altered modal shapes, which are critical in understanding the overall dynamic response.

5.3. Signal Propogation and Defect Categorization

In this section, main goal is to investigate how different structural defects in a spider-web model affect the propagation of an initial pulse (or "signal" as mentioned earlier in chapter 4) through the web. We developed two separate Python Model codes:

- Code 1 (Initial Approach): Implemented mild or local defects (e.g., a single missing node, a single missing edge, or one weakened edge) as in previous section with relatively higher damping and a weak restoring force to the equilibrium position.
- Code 2 (Revised Approach): Introduced *more dramatic* defects (e.g., removing an entire radial, removing the outer ring, weakening an entire inner ring), *reduced damping*, and *eliminated* the ground restoring force to emphasize the differences in dynamic response caused by the defects.

In both codes, the web is represented as a collection of nodes (with masses) and edges (with spring-like connections). The equations of motion are solved numerically using `solve_ivp` from the `scipy.integrate` package in Python. We track the displacement of a pulsed node over time and compare the time series and frequency domain (FFT) responses under different defect scenarios.

5.3.1. Initial Approach

- **Defects:** Single missing node, single missing edge, or a weakened edge.
- **Damping:** Moderately high ($c = 0.1$) so the system dissipates energy relatively quickly.
- **Ground restoring force:** A small k_r that pulls each node to its initial position.
- **Pulse:** A moderate impulse applied to one interior node.

In Fig 5.7, we plot the displacement magnitude at the pulsed node for the *Ideal Web*, the *Missing Node* case, the *Missing Edge* case, and the *Weakened Edge* case. Although some minor variations are visible, *all four curves largely overlap and decay to near zero by* $t \approx 15$ *s*. As shown in Figure 5.7, the frequency domain responses are also very similar.

That little difference is due the defects are small and localized (removing or weakening only a single node/edge), and because the damping is high enough to overshadow subtle structural differences. Additionally, restoring force (k_r) helps pull all nodes back to their equilibrium, further homogenizing the response. This indicate that spider webs are very efficient structures that capture energy losses due to their structure. This perfectly allings with conclusions made by different researchers that spider webs are very sustainible structures due their structure.

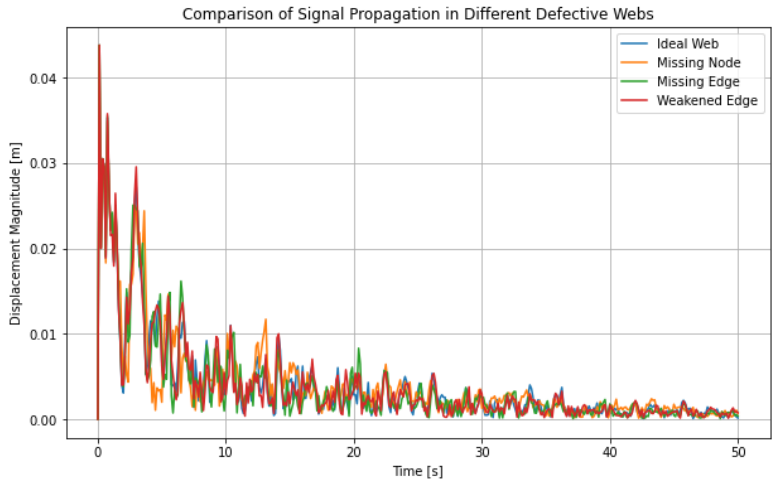

Figure 5.7: FFT comparison (Code 1): The amplitude spectra exhibit only slight differences among the four scenarios, indicating that mild defects and higher damping produce nearly indistinguishable responses.

5.3.2. Revised Approach

Since the initial approach did not reveal clear differences among defect categories, we introduced:

- More dramatic defects:
  1. Removing an entire radial (all nodes/edges along one spoke).
  2. Removing the outermost ring (affecting boundary conditions).
  3. Weakening all edges in a middle ring to only 10% of their original stiffness.
- Lower damping (e.g., $c = 0.02$) so oscillations last longer and differences in the structure have time to manifest.
- Stronger springs ($k = 200$) to increase the vibration amplitude, further amplifying structural differences.

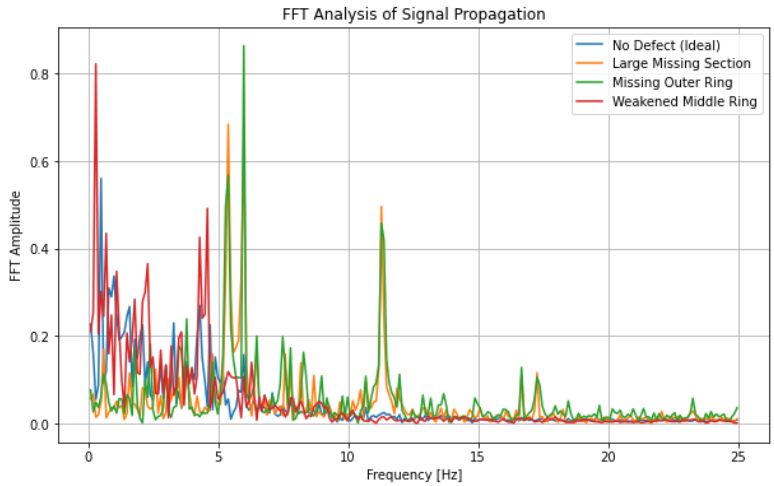

Figure 5.8: FFT comparison (Code 2): The new defect cases (large missing section, missing outer ring, weakened middle ring) now produce *distinct* frequency peaks and amplitudes compared to the ideal case. Lower damping reveals each web's unique vibration modes.

Figure 5.8 illustrates the FFT analysis for:

1. **No Defect (Ideal)**: Shows multiple harmonic peaks but a relatively smooth decay in amplitude at higher frequencies.
2. **Large Missing Section**: Removing one entire radial (spoke) creates a significant asymmetry. A new strong peak emerges around 3–5 Hz, indicating a shift in the natural frequencies.
3. **Missing Outer Ring**: The boundary is no longer intact, causing more pronounced lower□frequency modes and a strong peak near 2 Hz.
4. **Weakened Middle Ring**: Reducing stiffness in the middle ring alters intermediate modes, creating additional peaks in the 6–8 Hz range.

By combining larger defect areas (entire radial or ring removed/weakened), Lower damping, and no ground restoring force, we effectively magnify the impact of local stiffness/connectivity changes on the global vibration modes. Consequently, the signal propagation and energy decay exhibit clear differences for each defect scenario.

6

Discussion

This chapter critically revisits the main findings of the thesis, which explores signal propagation in spider web–like networks. While the report offers intriguing models and simulation results, an in-depth analysis of the underlying assumptions and methodologies reveals several areas of concern. This discussion expands on earlier critiques by incorporating detailed aspects from the document, aiming to interrogate every major component of the study.

6.1. Critical Review of Structural Models

The force distribution model is founded on a recurrence relation as in literature review, while mathematically elegant, relies on several idealizations:

- Homogeneity Assumption: The model assumes that the radial threads (with stiffness K) and spiral threads (with stiffness k) behave uniformly. In natural spider webs, however, thread diameters vary (e.g., radial threads are typically 2.67 to 5 μm versus 0.72 to 1.04 μm for spiral threads), leading to non-uniform stiffness and force propagation.
- Symmetry and Linearity: The recurrence relation implies a linear, additive force transmission along idealized, symmetric nodes. Real webs are irregular, and stress concentrations or nonlinear effects especially near damaged or defective areas may lead to deviations from these predictions.

6.2. Limitations of Signal Propagation Simulations

The thesis describes three distinct simulation methods for signal propagation:

Simple Collision Model

This model: Assigns fixed propagation velocities (e.g., 0.8 units/time for radial threads, 1.0 units/time for spiral threads) and employs a discrete time-step approach. While useful for highlighting general trends such as the high collision density near central nodes—the model's discretization may oversimplify the continuous dynamics of wave propagation, and the sensitivity to the chosen threshold undermines the robustness of its predictions.

Random Walk Study

In this approach: A large number of signals perform random walks on a network modeled after the web's geometry. Collisions are recorded when signals meet at nodes or along edges.

The stochastic nature of the model introduces variability that might mimic real-world signal dispersion, yet its physical basis is questionable. The absence of a rigorous derivation of transition probabilities or energy considerations limits the validity of the inferred collision statistics. Moreover, the scalability of the model is problematic, as increasing the number of signals or steps dramatically raises computational demands.

Wavefront Simulation

The most refined simulation method tracks signal packets continuously: Signal intensity is modeled with energy loss factors and adaptive transmission, while collision detection is based on proximity criterial. The simulation integrates physical properties such as tension and mass per unit length using the formula $|v| = \sqrt{F_t/\mu}$.

Despite offering a more detailed view of signal behavior, the method suffers from high computational overhead. Simplified assumptions in the merging criteria and energy decay model might lead to oversights in complex interference patterns and the role of environmental noise.

6.3. Appraisal of the Advanced Mass-Spring and Defect Models

The thesis extends the analysis by introducing an advanced mass–spring network model with defects. Key features include:

- Mass–Spring Network: Nodes are arranged on concentric rings, with forces computed via Hooke's law:
$$F_{ij} = -k\left(\|x_i - x_j\| - L_{ij}\right)\frac{x_i - x_j}{\|x_i - x_j\|}.$$
The numerical integration, conducted using a Runge–Kutta method with very tight tolerances, is designed to capture detailed dynamic behavior.
- Energy Dissipation and FFT Analysis: The simulation tracks total energy, demonstrating an exponential decay due to damping. FFT analysis is used to identify dominant vibrational modes, yet the sensitivity of FFT to numerical noise calls the reliability of the spectral peaks into question.
- Defect Modeling: Defects are introduced by randomly deactivating nodes and weakening edges. Although this stochastic approach mimics some aspects of natural imperfections, it lacks empirical grounding. The parameters (e.g., missing node probability, weakened edge factor) are chosen arbitrarily, making it difficult to assess their impact on network resilience without experimental validation.

6.4. Implications for Bio-Inspired Artificial Network Design

One of the central ambitions of the thesis is to draw parallels between spider web mechanics and the design of robust artificial networks. However, significant challenges remain:

- Scale and Material Discrepancies: Natural spider webs operate under biological constraints that differ markedly from engineered communication systems. The scale, material properties, and environmental interactions in engineered networks are not adequately addressed by the models.
- Extrapolation of Simplified Models: The insights from idealized force distribution and vibrational analyses may not translate directly into practical design guidelines. Without rigorous experimental data or more complex models accounting for nonlinearity and heterogeneity, the potential benefits of applying these principles to artificial networks remain speculative.

6.5. Conclusions and Recommendations for Future Work

While the thesis provides a framework for exploring signal propagation in spider web–like networks, every key finding warrants further research. The reliance on idealized geometries and linear, additive force laws simplifies the complex, heterogeneous nature of natural systems, and future models should incorporate experimental data on silk properties and web geometry. In addition, the three simulation approaches each have limitations, refining these models to include continuous dynamics, realistic energy dissipation, and non-randomized physical parameters would enhance their predictive capability. Experimental validation is crucial; comparing simulation outcomes with empirical observations from actual spider webs could help calibrate model parameters and validate the theoretical framework. Moreover, before the principles of spider web mechanics can inform artificial network design, a more comprehensive investigation into the scaling effects and material differences is required.

In summary, while the study makes a valuable contribution by attempting to bridge biological inspiration and network theory, its conclusions remain provisional. A more rigorous, validated approach is needed to confirm whether these bio-inspired models can indeed lead to robust, efficient artificial networks.

7

Conclusion

The thesis has explored the mechanics and signal propagation in spider web-like networks, combining theoretical analysis with numerical simulations to uncover key principles underlying their resilient design. By examining both static force distribution and dynamic signal behavior, we have gained a deeper understanding of how natural systems efficiently manage stress and interference, and how these ideas can inspire robust engineered networks.

The objective of the thesis was to explore how variations in velocity, geometry, and structural complexity influence both force distribution and dynamic behavior, and the results have provided several important insights into the design of resilient networks. The theoretical framework, established through recurrence relations and derived from the mechanical principles observed in natural spider webs, underpins the entire study. Through the thesis, only the network as a system where forces propagate from node to node, it was shown that the hierarchical arrangement characterized by stiff radial threads and flexible spiral threads ensures that stresses are effectively redistributed. This mechanism minimizes localized stress concentrations and preserves the structural integrity even under damage. The simulations confirmed that, as the stiffness ratio between radial and spiral elements increases, forces are distributed more evenly toward the periphery, thereby enhancing the system's overall robustness.

Dynamic simulations of signal propagation provided further insights. Three distinct approaches were employed: a discrete collision model, random walk, and a continuous wavefront simulation. In the discrete approach, the evolution of signals through the network revealed that central nodes, due to their high connectivity, consistently experience intense activity and a higher frequency of collisions. These collisions, which occur when multiple signal paths converge, serve as a natural mechanism for energy dissipation and interference management.

Building on this, the random walk study introduced a random walk method to simulate signal trajectories. By allowing signals to move in random directions across the network's predefined paths, this approach offered a complementary perspective on collision dynamics. Although less precise in tracking continuous signal behavior, the random walk model underscored the stochastic nature of signal propagation and provided evidence that even in seemingly chaotic movement, the central regions of the network consistently experienced higher collision densities. This reinforced the conclusion that network hubs are critical for understanding and optimizing signal transmission.

The most refined propagation model, the wavefront simulation, incorporated continuous tracking of signal packets with energy loss, merging of colliding packets, and detailed time evolution of the system. This method allowed for a precise quantification of how signals attenuate and interact over time, offering a deeper insight into the dynamics of interference and energy dissipation. The wavefront simulation not only confirmed the collision patterns observed in the simpler models but also revealed additional subtleties such as the effects of energy decay and the temporal evolution of collision events. The trade-offs between model resolution and computational cost were evident, with the wavefront approach providing high-fidelity results at the expense of increased simulation complexity.

In parallel to these studies, the advanced mass–spring network model provided a deeper understanding of the vibrational dynamics inherent to these structures. By applying an initial velocity pulse to a selected node and monitoring its displacement over time, the model captured the complex dynamics of wave propagation in a damped, nonlinear medium. The resulting time series exhibited an exponential decay in energy, consistent with the expected behavior of a dissipative system. Analysis through Fast Fourier Transform (FFT) further revealed distinct vibrational modes—peaks in the frequency domain corresponding to the fundamental and higher-order harmonics. These spectral features validate the model's ability to replicate the complex vibrational behavior of a spider web-like structure and provide insights into how damping and structural parameters influence the overall dynamic response.

The simulation of defects introduced an additional layer of complexity to the study. By modeling missing nodes, broken links, and irregular mass distributions, the research explored how imperfections affect the network's signal propagation. The results indicate that defects can lead to localized disruptions and alter the force distribution, yet the overall structure remains surprisingly resilient. This observation is in line with the biological inspiration from spider webs, where natural imperfections do not compromise functionality. Instead, these networks adapt dynamically to maintain efficient signal transmission despite damage or variability in material properties.

Overall, the findings of this thesis demonstrate that spider web-like networks embody a set of design principles that are both efficient and resilient. The combination of strong radial elements and flexible spiral connections provides an elegant solution for managing forces and minimizing the impact of damage. Although the models presented here involve certain simplifications and face computational challenges, they lay a solid foundation for future research.

Looking forward, several views for further investigation emerge. Enhancing computational methods—such as through parallel processing or improved numerical algorithms—could allow for more detailed and larger-scale simulations. Experimental validation, whether in the laboratory or in field studies of natural spider webs, would help confirm the theoretical predictions and simulation outcomes. Moreover, incorporating adaptive and stochastic elements into the models could yield a more realistic representation of natural variability, thereby refining our understanding of signal propagation under different conditions.

In conclusion, this research not only deepens our understanding of the mechanics behind spider web like networks but also highlights their potential as a source of inspiration for designing resilient communication, sensor systems and architecture.

Bibliography

[1] Han, S.I., Blackledge, T.A., & Bhamla, S. (2021). *Slingshot spiders build tensed underdamped webs for ultrafast launches and speedy halts*. Current Biology, 32(2), 240–248. https://pubmed.ncbi.nlm.nih.gov/33723624/

[2] University of Oxford (2020). *Good vibrations: spider signal threads reveal remote sensing design secrets*. https://www.ox.ac.uk/news/science-blog/good-vibrations-spider-signal-threads-reveal-remote-sensing-design-secrets

[3] Cranford, S.W., Tarakanova, A., Pugno, N.M., & Buehler, M.J. (2012). *Spider orb webs rely on radial threads to absorb prey kinetic energy*. Journal of The Royal Society Interface, 9(73), 3240–3248.

[4] Aoyanagi, Y., & Okumura, K. (2010). *Simple Model for the Mechanics of Spider Webs.* Physical Review Letters, 104(3), 038102. https://doi.org/10.1103/PhysRevLett.104.038102

[5] Lott, J., Tarakanova, A., & Buehler, M. J. (2022). *Prey Localization in Spider Orb Webs Using Modal Vibration Analysis*. Journal of the Royal Society Interface, 19(189), 20210868. https://doi.org/10.1098/rsif.2021.0868

[6] M. Lott, V. F. Dal Poggetto, G. Greco, N. M. Pugno, and F. Bosia, "Prey Localization in Spider Orb Webs Using Modal Vibration Analysis," *Scientific Reports*, vol. 12, no. 1, 2022. https://doi.org/10.1038/s41598-022-10662-8

[7] Merriam-Webster, Incorporated, "Dipteran," in *Merriam-Webster.com Dictionary*, Springfield, MA: Merriam-Webster, Incorporated. https://www.merriam-webster.com/dictionary/dipteran.

[8] North Carolina State University, "Order Diptera," in *General Entomology (ENT 425)*, Raleigh, NC: North Carolina State University. https://genent.cals.ncsu.edu/insect-identification/order-diptera/.

[9] Animal Diversity Web, "Musca domestica," in *Animal Diversity Web*, Ann Arbor, MI: University of Michigan. https://animaldiversity.org/accounts/Musca_domestica/

[10] ResearchGate: SEM Micrographs of Spider Web Components. https://www.researchgate.net/figure/SEM-micrographs-of-the-different-components-of-the-spider-web-Diameters-of-spider-sil fig2_331022410

[11] S. W. Cranford, A. Tarakanova, N. M. Pugno, and M. J. Buehler, *"Nonlinear material behavior of spider silk yields robust webs,"* Nature, vol. 482, pp. 72–76, 2012. [Online]. Available: https://doi.org/10.1038/nature10739

[12] A. Sensenig, I. Agnarsson, and T. A. Blackledge, *"Behavioral and biomaterial coevolution in spider orb webs,"* Journal of Evolutionary Biology, vol. 23, no. 9, pp. 1839–1856, 2010. https://doi.org/10.1111/j.1420-9101.2010.02048.x

[13] B. Mortimer, J. A. Gordon, and F. Vollrath, *"Dynamic Mechanical Properties of Spider Silks: Impact of Stiffness on Web Function,"* Journal of The Royal Society Interface, vol. 11, no. 98, 2014. https://doi.org/10.1098/rsif.2014.0258